

Neural Control of Rotational Kinematics Within Realistic Vestibuloocular Coordinate Systems

MICHAEL A. SMITH¹ AND J. DOUGLAS CRAWFORD^{1,2}

Centre for Vision Research and ¹Department of Psychology and ²Department of Biology, York University, Toronto, Ontario M3J 1P3, Canada

Smith, Michael A. and J. Douglas Crawford. Neural control of rotational kinematics within realistic vestibuloocular coordinate systems. *J. Neurophysiol.* 80: 2295–2315, 1998. Previous theoretical investigations of the three-dimensional (3-D) angular vestibuloocular reflex (VOR) have separately modeled realistic coordinate transformations in the direct velocity path or the nontrivial problems of converting angular velocity into a 3-D orientation command. We investigated the physiological and behavioral implications of combining both approaches. An ideal VOR was simulated using both a plant model with head-fixed eye muscle actions (standard plant) and one with muscular position dependencies that facilitate Listing's law (linear plant). In contrast to saccade generation, stabilization of the eye in space required a 3-D multiplicative (tensor) interaction between the various components of velocity and position in both models: in the indirect path of the standard plant version, but also in the direct path of the linear plant version. We then incorporated realistic nonorthogonal coordinate transformations (with the use of matrices) into both models. Each now malfunctioned, predicting ocular drift/retinal destabilization during and/or after the head movement, depending on the plant version. The problem was traced to the standard multiplication tensor, which was only defined for right-handed, orthonormal coordinates. We derived two solutions to this problem: 1) separating the brain stem coordinate transformation into two (sensory and motor) transformations that reordered and "undid" the nonorthogonalities of canals and muscle transformations, thus ensuring orthogonal brain stem coordinates, or 2) computing the correct tensor components for velocity-orientation multiplication in arbitrary coordinates. Both solutions provided an ideal VOR. A similar problem occurred with partial canal or muscle damage. Altering a single brain stem transformation was insufficient because the resulting coordinate changes rendered the multiplication tensor inappropriate. This was solved by either recomputing the multiplication tensor, or recomputing the appropriate internal sensory or motor matrix to normalize and reorthogonalize the brain stem. In either case, the multiplication tensor had to be correctly matched to its coordinate system. This illustrates that neural coordinate transformations affect not only serial/parallel projections in the brain, but also lateral projections associated with computations within networks/nuclei. Consequently, a simple progression from sensory to motor coordinates may not be optimal. We hypothesize that the VOR uses a dual coordinate transformation (i.e., both sensory and motor) to optimize intermediate brain stem coordinates, and then sets the appropriate internal tensor for these coordinates. We further hypothesize that each of these processes should optimally be capable of specific, ex-

perimentally identifiable adjustments for motor learning and recovery from damage.

INTRODUCTION

The purpose of this investigation was to explore the impact of neural coordinate transformations on the computations that occur *within* these coordinates, using the angular vestibuloocular reflex (VOR) as a case study. The function of the angular VOR is to stabilize the retinal image during head rotations. Ideally, this is accomplished by rotating the eye around the same axis as the head by an equal amount, but in the opposite direction. Experiments have shown that the VOR is capable of rotating the eye about any arbitrary axis (Angelaki and Hess 1994; Crawford and Vilis 1991; Curthoys et al. 1997; Hess and Angelaki 1997; Misslisch et al. 1994; Seidman et al. 1995; Simpson and Graf 1985; Solomon et al. 1997). Owing to the relative simplicity of this reflex, it has been simulated extensively; both with the use of neural network models, which attempt to address how neural computations occur within realistic patterns of connectivity (Anastasio and Robinson 1990; Robinson 1992), and with algorithmic models, which attempt to clarify the mathematical nature of these computations, and thereby generate experimental predictions to identify their input-output behavior in successively smaller "black boxes" (Merfeld 1995; Robinson 1982; Schnabolk and Raphan 1994; Tweed and Vilis 1987). The current investigation follows the latter of these two traditions.

Anatomically, the VOR can be broken down into three serial components: the canals, the extraocular muscles of the eye, and the active neural connections between them (Fig. 1). The six semicircular canals form three functional pairs that lie in planes roughly orthogonal to each other. In addition, each canal works in a reciprocal arrangement with its paired partner in a push-pull fashion (Galiana and Outerbridge 1984). The brain stem supplies the necessary neural connections and weightings to deliver the signals from the canals to the eye muscles to move the eyes appropriately for the VOR. These connections are affected through the "3 neuron arc": primary afferents from the vestibular canals carry a velocity signal that innervate the vestibular nucleus, the projections of which innervate the oculomotor nucleus, which in turn connects with the motoneurons of the eye. The final component of the VOR, the eye muscles, consists of six extraocular muscles for each eye. These six muscles are also arranged in three reciprocal pairs, the pulling direc-

The costs of publication of this article were defrayed in part by the payment of page charges. The article must therefore be hereby marked "advertisement" in accordance with 18 U.S.C. Section 1734 solely to indicate this fact.

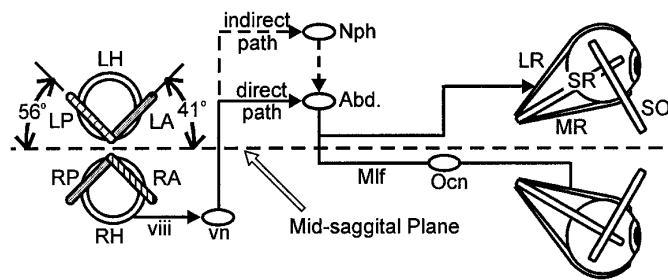


FIG. 1. Arrangement of canals and muscles. Canals: LA/RA, left/right anterior; LH/RH, left/right horizontal; LP/RP, left/right posterior; vn, vestibular nucleus. Shaded canals show push-pull arrangement. The right and left horizontal canals form 1 pair that lies roughly in the horizontal plane and is sensitive to horizontal head rotations. A 2nd pair is formed by the left anterior and right posterior canals, whereas the 3rd pair is formed by the right anterior and left posterior canals. The 2nd and 3rd functional pairs lie in vertical planes that are roughly orthogonal to each other and are rotated with respect to the saggital plane of the head. This arrangement allows these 2 pairs to be sensitive to both the vertical and torsional components of head motion (where torsion is defined as rotation about the nasal-occipital axis). Muscles: SO, superior oblique; SR, superior rectus; LR, lateral rectus; MR, medial rectus [the inferior oblique (IO), and inferior rectus (IR) lie directly under their superior counterparts and are not shown]. Middle section: schematic of brain stem pathways showing direct (velocity) and indirect (position) paths for horizontal VOR. Abd., abducens nucleus; Nph, nucleus prepositus hypoglossi; Mlf, medial longitudinal fasciculus; Ocn, oculomotor nucleus.

tions of which lie in approximately the same planes as the canals (Robinson 1982). As with the canals, the muscles also work in a reciprocal relationship. For example, a change in the balance of activity between the horizontal canals would lead to the appropriate change in torques between the medial and lateral rectus muscles to stabilize horizontal gaze direction.

In simulations of a one-dimensional (1-D) VOR, the velocity component of the motoneuron signal is carried by the direct path while the required position component of the signal is developed in an indirect path through the mathematical equivalent of integration (Robinson 1975). These two signals are then summed at the motoneurons and sent to the plant (a simulation of the eye globe, surrounding tissue, and musculature). At first glance, a 3-D VOR should simply be a triplication of this basic circuit (1 each for the horizontal, vertical, and torsional directions). This is not so, however, because two major complications arise in going from a 1-D VOR to a 3-D VOR. The first complication resides in the geometry of the canals and eye muscles themselves, whereas the second complication arises from the problems in generating the 3-D position signal from the 3-D angular velocity signal supplied by the canals (Tweed and Vilis 1987).

First, on close inspection, the canal/muscle planes are not perfectly orthogonal, and the alignment between the canal and the muscle planes is not perfect (Blanks et al. 1975; Simpson and Graf 1981). As a result, a set of single one-to-one direct path connections between the individual canals and muscles would not produce an ideal VOR (Pellionisz and Llinas 1980). An elegant solution to the problem of the differing canal and muscle orientations was supplied by Robinson (1982, 1985), where the orientation of the canals was represented with the use of a 3×3 matrix (C). That is, the values within the matrices represented the degree of

sensitivity of each canal to each component of head rotation. A similar matrix (M) was used to represent the eye muscle pulling directions, and a third brain stem matrix (B) was computed to represent the required connections between C and M. Although some have suggested that the brain stem might develop intermediate coordinate systems (Crawford 1994), the Pellionisz-Robinson approach has influenced many investigators to view the brain stem as a progressive transformation from sensory to motor coordinates (Pellionisz and Llinas 1980; Robinson 1992).

The second complication, that of generating a 3-D orientation signal from angular velocity, was addressed by Tweed and Vilis (1987). In that paper, they noted that 3-D orientation was not simply the integral of velocity (as it is in 1-D) because rotations in 3-D space are noncommutative (i.e., the order of the rotations matters). To solve this problem, their model used an internal feedback loop with a multiplicative interaction between the velocity signal (supplied by the canals) and the brain stem's estimate of current eye position. The resulting signal, a desired rate-of-change-in-eye-position, was then integrated to give the brain stem's estimate of eye position. However, some have recently suggested that if eye muscle pulling directions are rigged to have particular position dependencies, then the multiplicative stage in this model would not be necessary (Demer et al. 1995; Raphan 1997, 1998).

To date, these two approaches to modeling the VOR have remained separate, and a complete model of the VOR that uses realistic coordinate systems in both paths has been unavailable. Our first goal was to determine how plant characteristics affect the need for a multiplicative step in the VOR. Our second goal was to implement the resulting models in physiologically realistic coordinate systems, and in so doing, to explore some of the complications that might arise and their implications for VOR physiology, learning, and recovery from damage.

THEORETICAL BACKGROUND

Robinson's matrix model

CANAL MATRIX. In 1982, Robinson modeled the 3-D VOR by using matrices to represent the actions of the canals and muscles of humans and the neural connections between them, in stereotaxic coordinates. In his paper, Robinson defined a *canal sensitivity vector* to mean an oriented unit vector along the axis orthogonal to the plane of the canal. The projection of the component of head movement orthogonal to the plane of the canal onto the sensitivity vector represented that canal's response to each component of head velocity. Robinson defined such a sensitivity vector for each canal pair and so constructed the vestibular response to any head movement in terms of rotation vectors. Because Robinson's matrix model was 3-D, the neural response of each canal pair to a head rotation had three components. Taking the three canal pairs together, he constructed a 3×3 canal matrix. In the functionally equivalent matrix shown here (altered to fit our experimental coordinate system), each row corresponds to the neural response of a canal functional pair to a unit vector input, whereas the columns represent the

component response of each pair along the indicated axis of rotation (Robinson 1982)

$$\begin{matrix} & i & j & k \\ \text{Ralp} & \begin{bmatrix} 0.723 & 0.673 & 0.156 \end{bmatrix} \\ \text{Rpla} & \begin{bmatrix} 0.723 & -0.673 & 0.156 \end{bmatrix} \\ \text{Lrh} & \begin{bmatrix} -0.374 & 0 & 0.927 \end{bmatrix} \end{matrix}$$

Ralp is the right-anterior/left posterior functional pair, rpla is the right-posterior/left anterior pair, lrh is the left-right horizontal pair, and *i, j, k* form the torsional, horizontal, and vertical basis vectors for a standard right-handed coordinate system (defined further below). For example, the value at row 3, column 3 (0.927), represents the response of the horizontal canal pair to the horizontal component of a unit head rotation about the vertical (*k*) axis. The canal matrix taken as a whole transforms an input vector of head velocity to an output velocity vector in *canal coordinates*. Such matrices, then, produce a transformation from one coordinate system to another. The values in our simulation matrices are the same as those used by Robinson (1985). It should be noted, however, that our conventions for indicating axes of rotation follow those of Tweed and Vilis (1987) rather than Robinson's *x, y, z*, notation (see METHODS), resulting in a different ordering of the matrix components.

MUSCLE MATRIX. The axes of rotation contributed by the eye muscles may also be represented in a 3×3 matrix because we have three functional pairs of muscles controlling three axes of rotation (assuming, for the moment, that the axes controlled by the muscles are head centered and independent of eye position). Robinson also constructed such a muscle matrix, the functional equivalent of which is shown below. This matrix transforms a vector in muscle coordinates to one in stereotaxic coordinates using data derived from anatomic studies (Blanks et al. 1975 as reported in Robinson 1982; and see Simpson and Graf 1981)

$$\begin{matrix} & \text{sio} & \text{sir} & \text{lmr} \\ I & \begin{bmatrix} 0.788 & 0.424 & 0.015 \end{bmatrix} \\ J & \begin{bmatrix} 0.6 & -0.906 & -0.005 \end{bmatrix} \\ K & \begin{bmatrix} 0.140 & 0.016 & 0.999 \end{bmatrix} \end{matrix}$$

Sio are the superior-inferior obliques, sir are the superior-inferior recti, lmr are the lateral and medial recti, and *i, j, k* represent the axis component axis of eye rotation. Note that the conclusions of the present study do not depend on the accuracy of this data, so long as it is generally representative. It should also be noted that the canal and muscle matrices are arranged with similar rows to minimize off-diagonal elements in the brain stem matrix (described below). However, because there is no inherent "order" between the canal or muscle pairs, the order of the rows is arbitrary. The order shown follows Robinson's (1982) choice and therefore will impose a left-handed coordinate system on the brain stem (the significance of which will be further discussed below).

BRAIN STEM MATRIX. Once the canal and muscle matrices have been established, it is a relatively simple matter to calculate the "brain stem" matrix required to take the values in the canal matrix to the values in the muscle matrix. To do this, Robinson noted that an ideal VOR requires an eye velocity vector that is equal to, but opposite to that of the head velocity vector. This overall result can be represented

as a negative identity matrix because such a matrix will maintain the integrity of the head velocity vector, but reverse its direction. Thus the three matrix multiplications are equal to the negative identity

$$MBC = -I \tag{1}$$

Upon rearranging the equation we have

$$B = M^{-1}(-I)C^{-1} \tag{2}$$

This provides a complete model for describing the input/output behavior of head/eye velocity in the ideal VOR. It should be noted that brain stem matrix values are calculated using canal and muscle data that were derived from anatomic data, whereas the overall metric is that of an ideal VOR. The equivalent matrix in our coordinates is shown here (conventions as before)

$$\begin{matrix} & \text{ralp} & \text{rpla} & \text{lrh} \\ \text{sio} & \begin{bmatrix} -0.919 & -0.267 & 0.212 \end{bmatrix} \\ \text{sir} & \begin{bmatrix} 0.212 & -0.997 & 0.146 \end{bmatrix} \\ \text{lmr} & \begin{bmatrix} -0.131 & -0.203 & -1.024 \end{bmatrix} \end{matrix}$$

Each entry can be conceived as the effective overall synaptic weightings from one canal pair (*top row*) to one muscle pair (*left column*).

As Robinson (1982) noted, canal and muscle damage could be simulated by altering their matrix values, which would, in turn, force the calculation of a new brain stem matrix (i.e., new neural weightings) to recover an ideal VOR. Such adjustments reflect the known plasticity of the VOR. For example, studies where the overall gain of the VOR has been altered by prism glasses (Gonshor and Melvill-Jones 1973) show that the neural weightings of the brain stem's connections have been adjusted to reestablish proper functioning.

3-D rotational kinematics

Robinson (1968) suggested that the brain stem must provide a position signal as well as a velocity signal through the equivalent of mathematical integration. The existence of such an integrator for horizontal eye movements was confirmed by behavioral measurements and was located and demonstrated, through physiological studies, to largely reside in the nucleus prepositus hypoglossi (Cannon and Robinson 1987; Cheron and Godaux 1987). Similarly, the integrator for torsional and vertical eye movements was found to include the interstitial nucleus of Cajal (Crawford et al. 1991).

The process of matching internal velocity and position signals was first explored in 1-D (Robinson 1975). In these models, a single value of horizontal head velocity representing a rotation of the head about a vertical axis was processed by both the velocity (direct) path and the position (indirect) path, and the resultant recombination of their outputs at the motoneurons elicited the correct response from the plant. Because these models were 1-D, the consequences of rotating bodies in 3-D space (mathematically described as rotational kinematics) were unseen for reasons outlined below.

A very brief summary of the implications of rotational kinematics for 3-D rotations is given here. For a more com-

plete treatment of the subject, see Tweed and Vilis (1987) or Haslwanter (1995). Henceforth the term “eye position” should be interpreted to mean “3-D eye orientation.” Gaze direction is said to have 2 degrees of freedom because it can be completely specified by two coordinates: one for horizontal position and one for vertical position. The eye, however, has 3 degrees of freedom because it can rotate around the gaze line (the 3rd degree of freedom) without changing the direction of gaze. During saccades, the 3rd degree of freedom is specified by Listing’s law. This law states that the eye will only assume orientations that can be reached from a selected reference position by a single rotation about an axis lying in a head-fixed plane. For one particular reference position, primary position, the line of sight is orthogonal to the associated plane, defined as Listing’s plane. Listing’s law has been confirmed for saccades and pursuit (Haslwanter et al. 1991; Straumann et al. 1991; Tweed and Vilis 1990). In contrast, the slow phase of the VOR will obviously violate Listing’s law if the head’s velocity axis has a torsional component with regard to Listing’s plane. However, even head rotation axes in Listing’s plane will cause torsional violations of Listing’s law as a function of initial eye position (Crawford and Vilis 1991). To see why this is so, we will first look at why saccades *obey* Listing’s law.

It has been well established that during saccades, if eye position is to stay in Listing’s plane (as required by Listing’s law), then the axis of rotation must tilt out of Listing’s plane for eye movements that are not toward or away from primary position (Tweed and Vilis 1990). It can be shown mathematically that, in such cases, the velocity axis must tilt out of Listing’s plane by half the angular displacement of the orthogonal component, the so-called half-angle rule. For example, a purely leftward 30° saccade beginning from an initial position of 40° up and 15° right, would require the velocity axis to tilt back out of Listing’s plane by 20° (½ the angle of vertical displacement). Mathematically, the relationship between eye position and velocity in 3-D is captured in the following equation

$$q = 2\dot{q}/\omega \quad (3)$$

where eye position (q) is expressed as a quaternion, \dot{q} is rate-of-change in eye position, and ω is the angular velocity vector of the eye (Tweed and Vilis 1987).

With VOR slow phases, however, the velocity axes ideally would not tilt out of Listing’s plane as a function of eye position, but rotate about the same axis as the head. Thus the ideal VOR does not employ a half angle rule.¹ As a result, eye position is forced out of Listing’s plane in a position-dependent manner. The consequence of violating Listing’s law, in an ideal VOR, is that eye position will accumulate torsional components during slow phases (in the

absence of torsion resetting quick phases (Crawford and Vilis 1991).

For such torsional eye positions to be held at the end of slow phases, a position signal would be required to oppose the elastic torque of the eye muscles that tries to restore eye position to its mechanically neutral state. However, because a VOR axis in Listing’s plane has no torsional component, the Robinson model cannot provide a torsional position signal through simple integration. Mathematically, the reason why this poses a problem for the Robinson model is because, in 3-D, eye position is not the integral of velocity. This fact is illustrated in Eq. 3, where \dot{q} (rate-of-change in position) is the derivative of q and, conversely, the integral of \dot{q} is q . It follows that, because ω does not equal \dot{q} (Eq. 3), it cannot be integrated to obtain q . Integration works in 1-D models of the VOR, because sequential rotations around a single axis do combine commutatively and additively, i.e., the order of movements does not matter. In 3-D, however, the order of rotations does matter, and the initial orientation is thus important in determining the final position (Quaia and Optican 1997; Tweed and Vilis 1987).

3-D Tweed/Vilis/Crawford model

A solution that accounts for the noncommutative nature of 3-D rotations was proposed by Tweed and Vilis (1987) and Crawford and Vilis (1991), when they suggested a velocity-to-position transformation that used a multiplicative step before integration. In their model, the brain stem’s command for eye velocity was first multiplied by a feedback copy of eye orientation to produce rate-of-eye-position change, which can be integrated. This model correctly predicted the position-dependent violations of Listing’s law. These predicted violations were investigated by Crawford and Vilis in 1991. In their paper, they showed that the VOR response of behaving monkeys followed a position-dependent pattern consistent with models that used the correct principles of kinematics, as suggested by Tweed and Vilis. Moreover, the position-dependent violations of Listing’s law held their positions, supporting the prediction of Tweed et al. (1994a) and contradicting a simple 3-D replication of the Robinson (1975) model and subsequent similar models (Schnabolk and Raphan 1994).

Recently, some investigators have suggested that plant mechanics could solve the rotational kinematics problem if position dependencies due to orbital “pulleys” implement the half-angle rule (Demer et al. 1995; Miller 1989; Raphan 1997, 1998). This has been demonstrated to be theoretically correct for the saccade generator (Crawford and Guitton 1997; Optican and Quaia 1998; Raphan 1998), but for the VOR the situation is less clear, because the VOR does not obey the half angle rule (Tweed 1997; Vilis 1997). Because the contribution of muscle mechanics to the position-dependent axis tilts required by Listing’s law are still a matter of some theoretical debate (Crawford and Guitton 1997), we employed two plant models to investigate any plant-dependent behaviors: a “standard plant,” which does not add any axis tilts (Tweed and Vilis 1987), and a “linear plant,” which fully implements the axis tilts (Crawford and Guitton 1997; Tweed et al. 1994a). The latter has been shown to

¹ Misslisch et al. (1994) found that the velocity vectors associated with pitch and yaw rotations tilted out of Listing’s plane by a quarter-angle rule rather than a half-angle rule during a VOR conducted by humans in the dark. Because previous theoretical investigations have assumed an ideal VOR (Robinson 1982) and the effects of species and vision (e.g., Solomon et al. 1997) are not yet clear, we will continue to simulate an ideal “zero angle” rule for simplicity and readdress this issue in the DISCUSSION.

provide an accurate approximation of the pulley model suggested by Raphan (1997), as shown by Optican and Quaia (1998).

Purpose and hypotheses of present investigation

Although the Tweed-Vilis-Crawford model produced appropriate 3-D VOR behavior (including violations of Listing's law) by correctly using the principles inherent in 3-D kinematics, the model was physiologically unrealistic because it used orthogonal coordinate systems in its calculations and did not address the possibility of a purely mechanical implementation of the half angle rule. Thus, our aim was 1) to determine the necessity of the multiplicative step with *both* plants and 2) to combine the resulting models with the realistic coordinates used by Robinson. First, we hypothesized that muscle mechanics cannot obviate the need for an internal multiplicative comparison between eye position and velocity in the VOR, because fundamentally, the input to the VOR is angular velocity, whereas the output is eye orientation. Second, we hypothesized that this comparison might not function correctly in arbitrary coordinates, making a trivial matrix-quaternion combination problematic. Finally, we hypothesized that any aspect of motor learning that impacts on neural coordinates would have to take into account the relationships between the computations occurring within those coordinates.

METHODS

Coordinate system

Eye velocities and orientations were simulated in a head-centric, right-handed, orthonormal coordinate system with the following basis vectors: i (axis for torsional rotations), j (horizontal axis for vertical rotations), and k (vertical axis for horizontal rotations). Rotations around these basis vectors were described using the right-hand rule as illustrated in RESULTS. Note that, this is distinct from the notion of a right-handed coordinate system that implies that, when pointing the right thumb along the first axis (e.g., $+i$) the fingers curl from the $+j$ axis to the $+k$ axis. The term orthonormal means that these coordinate vectors were mutually orthogonal and each were of length 1. These definitions are all important in understanding the results of this study.

To simplify our description of the 3-D VOR, we arbitrarily aligned our coordinates with the stereotaxic planes of the head. In addition, because the orientation of Listing's plane varies with respect to the head (Crawford 1994; Tweed and Vilis 1990), we made the simplifying assumption that it was aligned with the coronal plane, such that stereotaxic coordinates equated with Listing's coordinates. A more complete description of the VOR would require translational (Paige et al. 1996) and inertial coordinate transformations (Angelaki and Hess 1994), but this was beyond the scope of the current investigation.

QUATERNIONS. Quaternions were used to implement our models for two reasons. First, the previous Tweed-Vilis model (Tweed and Vilis 1987) used quaternions, and because we were combining this model with a matrix representation, we elected to maintain continuity by also using them. Second, quaternions are often easier to work with than most other representations, especially for very large rotations (Haslwanter 1995; Tweed and Vilis 1987).

Quaternions are mathematical constructs that consist of four elements (0–3) that can be thought of as a 3-D vector (elements

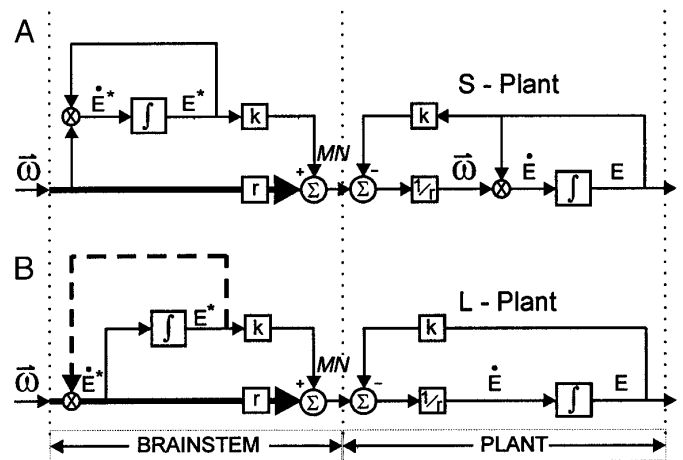


FIG. 2. Slow phase generator and 3-dimensional (3-D) oculomotor plant. *A*: standard plant (SP) model. A velocity signal proportional to the angular rotation of space relative to the head outputs from the canals (ω). The signal is relayed to the motoneurons (MN), and a velocity to position transformation within the indirect path, where ω is multiplied by the tonic output of the integrator. Output is estimated change-in-eye-position signal (E^*), which is then integrated (brain estimate of current-eye-position, E^*). Signals from these paths are summed at the motoneurons and output to the plant (see text for plant equations). *B*: linear plant (LP) model. The situation is similar to the standard model except that the direct path now propagates an estimated change-in-eye-position signal (E^*) rather than an eye velocity signal. The indirect path integrates the change-in-eye-position signal, and the resulting estimate of current-eye-position (E^*) is summed with (E^*) at the motoneurons (MN).

q_1 – q_3) together with a scalar (element q_0). The representation of angular rotations using quaternions is defined by

$$q_0 = \cos(\alpha/2) \quad (4)$$

and

$$q = \sin(\alpha/2)n \quad (5)$$

where n is a 3-D unit vector parallel to the axis of rotation (q); and α is the magnitude of the rotation. Although q already describes both the axis and magnitude of the rotation, q_0 becomes important in certain operations such as quaternion multiplication (Tweed and Vilis 1987). These angular rotation vectors (q_1, q_2, q_3) resemble the vectors in Fig. 3A. Where q_0 appears in models of brain stem function, it can be conceptualized as representing general neural redundancy (Tweed and Vilis 1990) rather than a separate neural channel.

Models

Crawford and Vilis (1991) and Tweed et al. (1994b) have measured actual VOR matrices in monkey and humans, respectively, and found them to be less than ideal (particularly in torsion). Nevertheless, for simplicity we chose to model an ideal, monocular, angular VOR for a distant target using two models (Fig. 2) that utilized quaternions to represent all kinematic variables.

In addition to combining the approaches of Tweed and Vilis (1987) with Robinson (1982), we also tested two different plants to determine whether the type of plant used would modify the resultant behavior: 1) a position-independent torque plant Fig. 2A (Tweed and Vilis 1987), in which muscle torques are fixed in the head (the standard plant model), and 2) a linear plant (Fig. 2B), which implements the position-dependent axis tilts observed in saccades (Crawford and Guitton 1997; Tweed et al. 1994a). The

standard plant can be described with the following equation (Tweed and Vilis 1987)

$$\mathbf{m} = k\mathbf{E} + r\boldsymbol{\omega} \quad (6)$$

whereas the linear plant input was described by Tweed et al. 1994

$$\mathbf{m} = k\mathbf{E} + r\dot{\mathbf{E}} \quad (7)$$

where \mathbf{m} is the motoneuron signal, k is the scalar elasticity constant, r is the scalar viscosity constant, \mathbf{q} is the eye position, $\dot{\mathbf{q}}$ is the rate of change in eye position, and $\boldsymbol{\omega}$ is the canal velocity vector (r and k can also be regarded as the matrices R and K with r and k , respectively, repeated along the main diagonal (Crawford and Guitton 1997).

CONTROL SYSTEM FOR STANDARD PLANT. The input of the standard plant model (Fig. 2A) was a velocity vector, $\boldsymbol{\omega}$, which represented the canal activity vector. This vector was divided by two to satisfy quaternion conventions and then sent down two parallel paths: the direct path (thick line) and the indirect path (thin lines). The direct path merely multiplied $\boldsymbol{\omega}$ by a scalar viscosity constant (r). The indirect path, however, supplied the position portion of the signal for the plant and therefore integrated the supplied velocity vector. To accomplish the required integration while at the same time obeying the rules of rotational kinematics, the velocity vector was multiplied by an estimate of current eye position (feedback from the brain stem integrator)

$$\dot{\mathbf{E}}^* = \boldsymbol{\omega}^* \mathbf{E}^* \quad (8)$$

using the standard formula for quaternion multiplication (Tweed and Vilis 1987; Westheimer 1957)

$$\begin{aligned} \dot{\mathbf{E}}_0^* &= \omega_0 \mathbf{E}_0^* - \omega_1 \mathbf{E}_1^* - \omega_2 \mathbf{E}_2^* - \omega_3 \mathbf{E}_3^* \\ \dot{\mathbf{E}}_1^* &= \omega_0 \mathbf{E}_1^* + \omega_1 \mathbf{E}_0^* + \omega_2 \mathbf{E}_3^* - \omega_3 \mathbf{E}_2^* \\ \dot{\mathbf{E}}_2^* &= \omega_0 \mathbf{E}_2^* + \omega_1 \mathbf{E}_0^* - \omega_1 \mathbf{E}_3^* + \omega_3 \mathbf{E}_1^* \\ \dot{\mathbf{E}}_3^* &= \omega_0 \mathbf{E}_3^* + \omega_1 \mathbf{E}_0^* + \omega_2 \mathbf{E}_2^* - \omega_2 \mathbf{E}_1^* \end{aligned} \quad (9)$$

where \mathbf{E}^* is treated as the right multiplied quaternion (Westheimer 1957). Note that $\boldsymbol{\omega}(0) = 0$ so that the first column of Eq. 9 can be eliminated in practice. The resultant quaternion $\dot{\mathbf{E}}^*$ is the derivative of \mathbf{E}^* , or a rate-of-change in orientation signal. This result was integrated component-wise (where i runs from 0 to 3)

$$\mathbf{E}_{(i)}^* = \int \dot{\mathbf{E}}_{(i)}^* \quad (10)$$

The resulting signal is an internal estimate of eye position (\mathbf{E}^*), which was then multiplied by the scalar elasticity constant (k). The signals from both paths were then summed component-wise at the motoneurons (Eq. 6). This signal was sent to the plant where current eye position (scaled by the elasticity constant, $k\mathbf{E}$) was subtracted. After removal (by division) of the viscosity constant (r), we were left with the original eye velocity vector ($\boldsymbol{\omega}$). This vector was then multiplied by current eye position (Eq. 8), resulting in a change of position value ($\dot{\mathbf{E}}$), the integration of which produced the new eye position (\mathbf{E}). This model was identical to the model proposed by Tweed and Vilis (1987) and used by Crawford and Vilis (1991). We will henceforth refer to this as the SP (standard plant) model.

CONTROL SYSTEM FOR LINEAR PLANT. Figure 2B, shows the model that employs a 3-D linear plant (Crawford and Guitton 1997; Tweed et al. 1994a). The motoneurons of the linear plant specify $\dot{\mathbf{E}}^*$ (the brain stem's estimate of the rate of change in eye position) in their phasic component, independent of eye position. This input simplifies saccade generation, but the implied position

dependencies required by Listing's law must, in effect, be "undone" in the VOR. Mathematically this required conversion of $\boldsymbol{\omega}$ to $\dot{\mathbf{E}}$ by a multiplicative feedback loop (Fig. 2B, dashed lines) common to both paths. This means that the direct path outputs a rate-of-position-change signal rather than the velocity signal as in the SP model. Thus the brain stem was changed to reflect the needs of the plant (Tweed 1997). We will henceforth refer to this as the LP (linear plant) model.

MATRIX TRANSFORMATIONS. It is into these two models (the SP and LP models) that we incorporated the realistic vestibular, brain stem, and eye muscle coordinate transformations in the form of matrices. These matrices were functionally the same as Robinson's, with the exception that they were reordered to fit our coordinates (i, j, k) and the following minor point. Robinson modeled the canal afferent vector as encoding head velocity relative to space. It may seem difficult to reconcile this with the fact that the vestibular sensors (and canal coordinates) are fixed with respect to the head. Furthermore, this requires that the canal vector be trivially multiplied by $-I$ (implicit in the brain stem matrix and thus the projection patterns to the muscles) to compute desired eye velocity for the VOR (Robinson 1982). This became particularly cumbersome when we employed more than one brain stem matrix (see RESULTS) and had to arbitrarily decide where to put the negative identity matrix. However, we eliminated this trivial problem by reinterpreting the canal vector as encoding space velocity in head coordinates, requiring a slight modification of Eqs. 1 and 2 such that the brain stem matrix was computed to give an overall VOR matrix equaling I . Finally, we sometimes altered certain elements of the C and M matrices (as described in RESULTS) to test Robinson's (1982) assertion that muscle or canal damage could be corrected by simply recalculating the brain stem matrix.

RESULTS

Ideal VOR response of the quaternion models

The following sections present results that are representative of the general properties observed in our simulations. For consistency, standard simulations conducted over five different initial eye positions in response to a constant velocity, rightward head movement of $100^\circ/\text{s}$ in the horizontal stereotaxic plane for a duration of 0.5 s are presented.

Figure 3 shows the ideal behavior of the VOR as simulated by the SP model, provided here as a control. A shows the eye and head velocity vectors (axes of rotation) during the movement, whereas B-E show position traces of the eye with respect to the head. Rotations represented in this and subsequent figures follow the right-hand rule. That is, if the thumb of the right hand is pointed in the same direction as the vector, then the curl of the fingers will give the direction of rotation indicated by that vector. For example, pointing the thumb of the right hand in the direction of the positive k axis of Fig. 3A (the axis of eye rotation), gives a finger curl indicating a leftward eye rotation. The position traces (Fig. 3B), numbered 1-5, correspond to an initial vertical eye position of 30° down, 15° down, 0° , 15° up, and 30° up, respectively. Each simulation began with the eye positioned 25° to the right. Thus, *simulation 1* began with an initial eye position of 25° right and 30° down with respect to the head. If the reader uses the right-hand rule (point the thumb in the direction of any one position i.e., toward the \odot symbol), *trace 1* of the behind view will indicate a leftward rotation of the eye in response to a rightward rotation of the head.

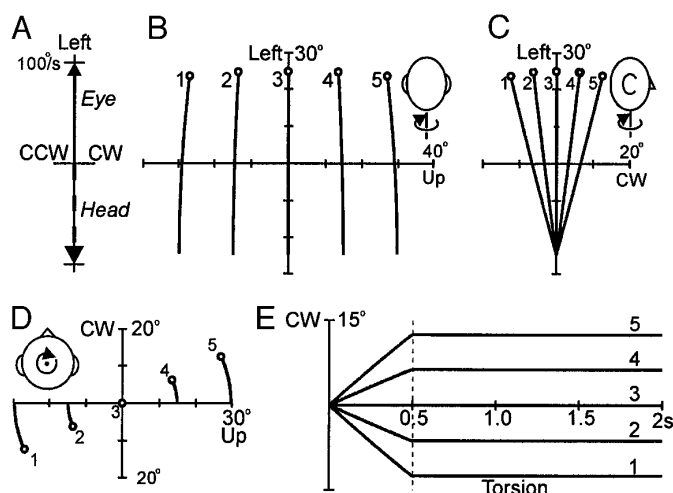


FIG. 3. Correct response of an ideal vestibuloocular reflex (VOR). Figure shows velocity vector and position traces (eye in head) of an ideal VOR from 5 different initial eye positions as output by both models. All initial horizontal eye positions began 25° to the right with respect to the head while initial vertical position varied as indicated: 1– 30° down; 2– 15° down; 0° to straight ahead at primary position; 4– 15° up; 5– 30° up). A: velocity vector of canal (—) and head (---). B: view from behind the simulated subject, showing the vertical and horizontal position traces. C: side view showing the direction and magnitude of torsion as a function of horizontal position. Note that this torsional pattern is required to generate correct 3-D eye orientation. D: torsional/vertical trace seen from above. E: torsion over time, showing that torsion is held constant and indefinitely at the end of head movement.

The other traces and views can be similarly assessed, with the exception of the torsion versus time trace (Fig. 3E).

In the view from behind the “subject” (Fig. 3B), the horizontal and vertical components of eye position are visible. These traces indicate that, not surprisingly, eye position mainly changed in the horizontal direction. As required for an ideal VOR, the eye held its final position (○) when the head stopped moving. In Fig. 3, C and D, the torsional component of eye position is visible. Here, Listing’s plane is aligned with the vertical axis (C) or the horizontal axis (D).

Note that in traces 1, 2, 4, and 5, a position-dependent torsional shift out of Listing’s plane occurred. These torsional components of eye position were seen even though the velocity vector was always within Listing’s plane (Fig. 3A) and therefore does not specify a torsional component. This was the result of the multiplicative component within the models, which accounted for the noncommutative nature of rotations (discussed above). When the eye began moving from an initial down and right position (1, 2), counterclockwise (CCW) torsion increased, whereas clockwise (CW) torsion was seen to build when the initial position of the eye was up and to the right (4, 5). Trace 3, however, showed no torsional increase because the eye moved across primary position. These results agree with the pattern of eye movements described by Crawford and Vilis (1991) and are required for perfect stabilization of the retinal image.

Figure 3E shows torsional behavior over time. Torsion continued to build until the head stopped moving (dashed vertical line) and then held, as observed experimentally (Crawford and Vilis 1991). It is evident from E that, if

torsion remained uncorrected, it would continue to build until the mechanical limits of the eye muscles were reached. Torsion does not normally build to such large levels or hold indefinitely during a real VOR because of the torsion-resetting aspect of the intervening quick phases (Crawford and Vilis 1991). Although these kinematically correct simulations in Fig. 3 were obtained from the SP model, our LP model (Fig. 2A) produced identical traces, because both models incorporated a 3-D multiplicative operation, but in different configurations (Fig. 2). We then evaluated the biological importance of this operation to the behavior of each model.

Contribution of the multiplicative component

Several investigators (Schnabolk and Raphan 1994; Straumann et al. 1995) have hypothesized that a multiplicative interaction is not required to handle 3-D rotations, but that a linear Robinson-style integrator is sufficient, especially if the eye plant could implement the axis tilts observed in saccades (Demer et al. 1995; Raphan 1997, 1998).

To directly test this hypothesis, we removed the multiplicative component from both the LP and SP models and then reassessed their performance. Figure 4 shows the results obtained with both the SP (—) and LP models (· · ·). Figure 4, A–C, shows eye position in head. The models no longer simulated an ideal VOR (see Fig. 3). With the SP model (—), the view from behind the subject (A) shows good performance in the horizontal and vertical directions, although the final position is not as accurate and there was some drift (at the cessation of head movement) that increased with eccentricity from primary position. The extent of this drift is seen more clearly in the side view (B). Eye position in head shows an incorrect torsional pattern (compared with Fig. 3C), which did not hold at the end of head movement but rather moved back into Listing’s plane (viewed edge on along the ordinate axis) as in the linear control model of Schnabolk and Raphan (1994). The LP model shows a similar pattern in Fig. 4A but produced a dramatically different pattern of torsional eye position. Figure 4C shows that the LP model trace always stayed in Listing’s plane (along the vertical axis). Note that the final torsional resting position simulated by both models was identical. Thus the response of both “linearized” models was incorrect, in the sense that they did not provide the eye-in-head torsional pattern seen in the ideal (Fig. 3) or real VOR (Crawford and Vilis 1991).

At first glance, this may seem like a somewhat trivial problem, but these head centric torsional errors disrupted the primary visual functions of the VOR. Figure 4, D–F, shows the functional implications of these errors. In D, both the SP model (—) and the LP models (· · ·) failed to hold a stable torsional eye position in space as required of an ideal VOR. Moreover, because these torsional errors do not correspond to rotation about the line of sight, they also destabilized 2-D gaze direction in space (E). Such eye movements would thus cause images to move with respect to the retina. The potential reduction in acuity will depend on eye velocity in space. In the real system, retinal image slip of more than $\sim 2.5^\circ/\text{s}$ (shown in F as a circle around

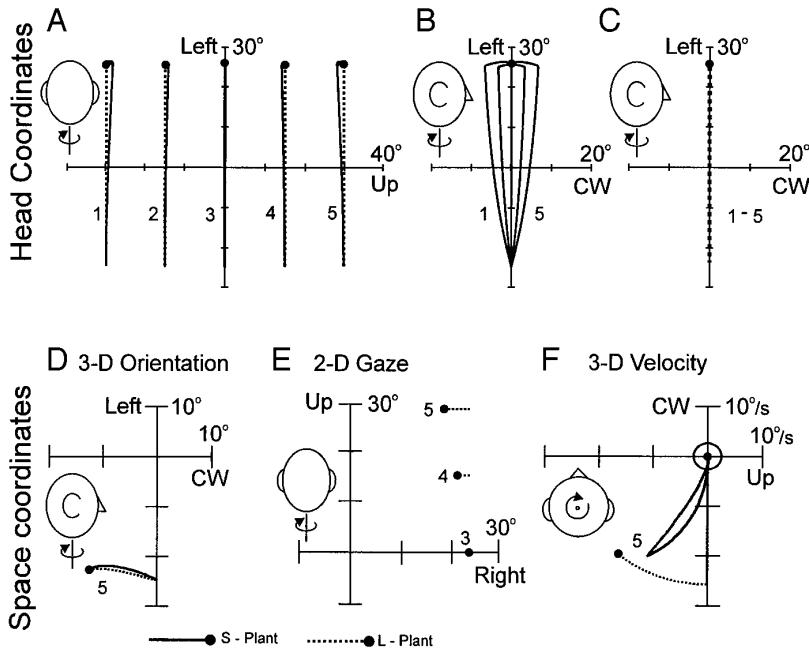


FIG. 4. Output of the quaternion models without the multiplicative component in response to a rightward head rotation of $100^\circ/\text{s}$ for 0.5 s . —, SP model; ···, LP model. ●, final eye position. The circle around the origin in *F* indicates region of foveal image stability ($2.5^\circ/\text{s}$). *A*: behind view of eye position in head (torsion/horizontal) SP model. Note that final torsional position incorrectly drifts back to Listing's plane. *C*: side view of eye position in head (torsion/horizontal) for simulations 1–5 (see Fig. 3). Note that torsion incorrectly remains in Listing's plane. *D*: side view of torsional/horizontal eye position in space. *E*: behind view of gaze in space (unstable) for LP model (SP model not shown because traces would mostly overlap). *F*: above view (torsion/vertical) of eye velocity in space.

the origin) has been shown to be detrimental to perception (Westheimer and McKee 1975). Eye velocity in space with the SP model (*F*, —) showed a peak magnitude of $\sim 20^\circ/\text{s}$ for trace 5. When the head stopped, velocity dropped back toward $0^\circ/\text{s}$ at a rate consistent with the time constant of the plant. The LP actually produced a higher eye velocity in space (*E*, ···) than the standard plant ($26.4^\circ/\text{s}$ vs. $20^\circ/\text{s}$) because all of its eye motion occurred during head movement. Thus both models showed an inability to hold correct eye position or gaze direction in space and produced retinal slip that was well beyond the acceptable limits of the real system. Indeed, the linear VOR controller actually produced greater errors driving the ‘‘pulley-equipped’’ linear plant than the standard plant.

We then computed the degree of retinal slip (quantified as eye velocity in space) for both models over a realistic range of horizontal head rotation speeds ($0\text{--}200^\circ/\text{s}$) and vertical eye positions ($10\text{--}40^\circ$) as depicted in Fig. 5. Figure 5*A* shows the results of the SP model, whereas *B* shows the results of the LP model. Both plants show increasing retinal slip with increasing displacement from primary position and increasing head speed. However, the LP model showed approximately twice the retinal slip as the SP model. Thus the multiplicative component is necessary for controlling both plants and is even more important for the linear plant. Having established that the multiplicative step is necessary for ideal behavior in both models, we then examined the performance of these models (see Fig. 2) in physiologically realistic coordinates.

Failure of the control system in realistic coordinates

For illustrative purposes, we initiated this study with a naive combination of the models simulated above with the Robinson-style matrix model. Figure 6 shows the standard configuration initially used to incorporate realistic coordi-

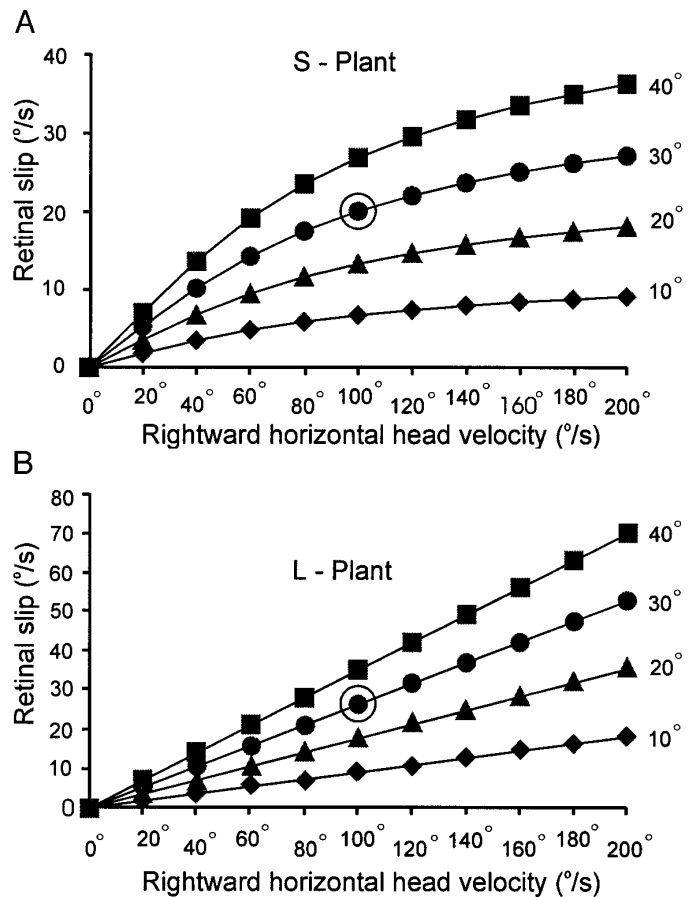


FIG. 5. Eye velocity in space without the multiplicative component as a result of different head rotation speeds. Ideally eye velocity in space should be $0^\circ/\text{s}$ to eliminate retinal slip. *A*: linear plant model. *B*: standard plant model. Data are plotted with 4 different initial vertical eye positions ($10, 20, 30,$ and 40°) down, respectively. ○, around the 2 data points indicate simulation 5 (depicted in Fig. 4*F*).

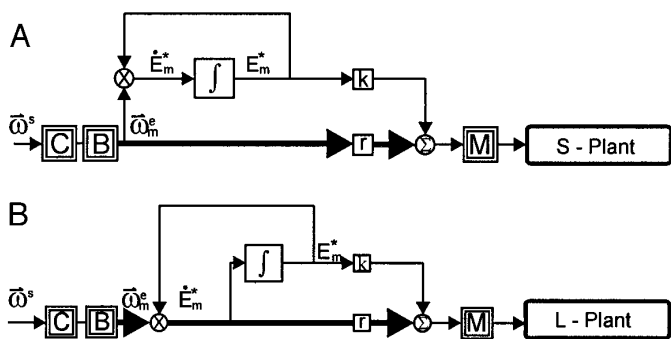


FIG. 6. Standard placement of coordinate transformations in models. A: SP model. Thick line, direct path; thin lines, indirect path. All vector quantities are represented by quaternions (i.e., $q1, q2, q3$). C, canal matrix; B, brain stem matrix; M, muscle matrix. ω is multiplied (using standard vector-matrix product) by the canal and then the brain stem matrix. The resultant signal is processed by both the direct and indirect paths. The summed result of these 2 paths is multiplied by the muscle matrix. B: LP model. Diagram conventions and values are the same as in A.

nates into our models. As predicted, the trivial combination of the correctly operating models with realistic coordinates in the form of canal, brain stem, and muscle matrices (SP matrix and LP matrix) failed to produce a correct response.

A characteristic pattern of errors was observed depending on the plant model. Figure 7, A–C, shows the results obtained with the standard plant, whereas D–F illustrate the results achieved using the linear plant. The solid lines indicate the now incorrect response of the models, whereas the dashed lines indicate the ideal response (a convention used in all diagrams from this point forward). Only standard simulations 3–5 are illustrated because simulations 1 and 2 are mirror images of 4 and 5. The behind view (Fig. 7A) shows only a slight positional error for the SP-matrix model in simulations 4 and 5. However, the above view (B) illustrates that incorrect torsional movement was observed with increasing eccentricity from primary position, both before and after the head stopped moving. This temporal behavior can be more clearly seen in Fig. 7C, where the vertical line indicates when the head stopped moving. At the cessation of head movement, the rate of positional deviation increased dramatically but then slowed as the eye approached its final resting position, showing an exponential decay at the intrinsic time constant determined by the plant (k/r).

In simulations with the LP-matrix model (Fig. 7, D–F), position traces showed a different pattern of errors. Vertical and horizontal position (D) were similar to those observed in the ideal VOR except that horizontal position was slightly less than ideal. However, the above view (E) shows that torsion moved immediately in the wrong direction. That is, instead of specifying CW torsion as required by an ideal VOR (---), the system specified CCW torsion. As in the ideal VOR, torsion increased during head movement and then held after the head stopped moving, but in the opposite direction. However, no torsional change (or any other positional change) was observed after the head ceased to move, although the final resting positions were the same for both models.

To further quantify the biological impact of these problems, we computed the velocity of retinal slip as described

above. Initially, we allowed the models to run freely (not shown) at 5 different head velocities 100, 200, 300, and 400°/s for a period of 0.5 s each. The problem of retinal slip increased with increasing head speed for both models. The SP-matrix model reached retinal slip velocities of 22–90°/s for the low to high end head rotation speeds, whereas the LP-matrix model produced retinal slip velocities that were approximately twice these magnitudes. Thus these models failed to emulate a VOR that was biologically realistic, let alone ideal. As we shall see, this was a result of two related computational problems that are both biologically problematic.

Further simulations isolated the problem to the multiplication tensor

Because the quaternion models without matrices produced a correct VOR response, it was the combination of those models with the matrices (representing realistic coordinates) that was problematic. Clearly the placement of one or more of these matrices was disrupting one or more of the compo-

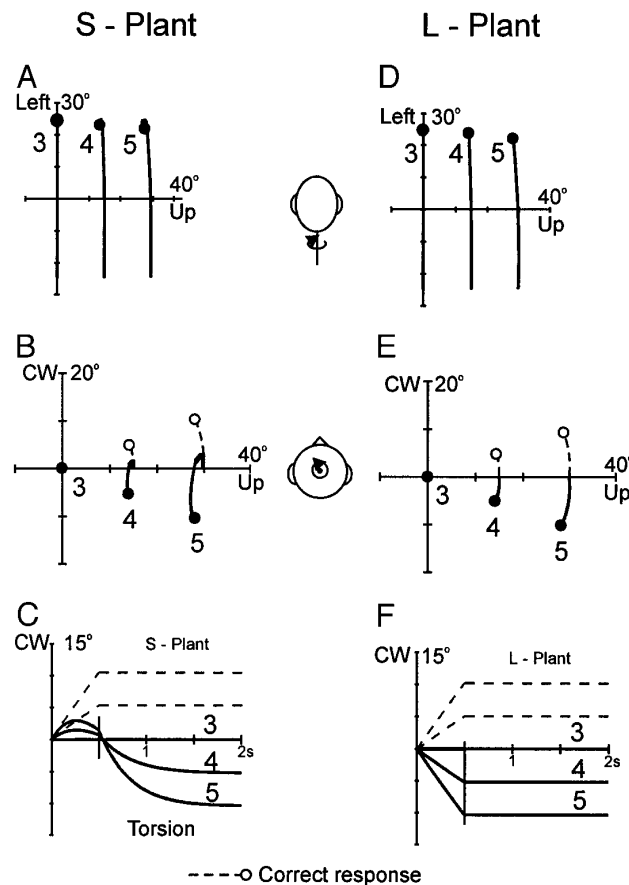


FIG. 7. Response of quaternion model with realistic coordinate systems (eye in head) to a rightward head rotation of 100°/s for 0.5 s. Top row: SP-matrix model. Bottom row: LP-matrix model. Correct response (dashed lines), incorrect response (solid lines). A and D: behind view of horizontal/vertical eye position in head. B and E: above view of torsion/vertical eye position in head. C and F: time/torsion. Numbered traces correspond to the same simulations seen in Fig. 3. Neither model produced the correct response.

nents of brain stem processing (because all matrix placements were upstream of the plant, plant operations remained unchanged). To confirm our hypothesis that the problem was isolated to the multiplicative operation, we manipulated the placement of the matrices so that different combinations of the internal operations were in orthogonal or physiological coordinates.

Figure 8 shows variations of the SP-matrix model, and representative simulations of each configuration [the same tests were also conducted with the LP-matrix model (not shown) with analogous results]. *Column 1* represents the various placement of matrices, *column 2* indicates torsional eye position relative to the head over time, and *column 3* shows eye position in space (as a measure of retinal slip). For reference, we have provided the control response (*row A*) as well as the response with our original matrix placement (*row B*), with the brain stem in motor coordinates. In *row C* we arranged the matrices differently to place the brain stem in sensory coordinates. This ordering represents another possible physiological arrangement, but the result was nearly indistinguishable from *row*

B. Thus our brain stem model malfunctioned in either motor or sensory coordinates.

We next moved to mathematical tests that did not represent physiological arrangements, but isolated the source of the errors. First, we put the multiplicative component in canal coordinates and left everything else in orthogonal coordinates (Fig. 8*D*). Again, the results were incorrect and virtually indistinguishable from *rows B* and *C*. Thus conducting the multiplicative step in canal coordinates and everything else in orthogonal coordinates still did not resolve the problem. This suggested that the problem was with the multiplicative vector operation. To confirm this, we conducted the multiplication in orthogonal coordinates while everything else was conducted in canal coordinates (*E*) according to the illustrated scheme. This time, the result was identical to the control. Thus only the multiplicative component was sensitive to the internal coordinate system.

Malfunctioning of the multiplicative component explained the differences between the responses in the two models. Because this step was confined to the indirect path of the SP model, its malfunction produced a pulse-step mismatch (Fig. 7*C*), whereas the malfunction of this step in both paths of the LP model produced an inappropriately directed but properly matched response (Fig. 7*F*). Our results illustrate that linear operations such as integration and scalar multiplication can be correctly performed in an independent piecemeal fashion on any individual component within a coordinate system without adversely affecting the other components. In contrast, the multiplication of eye velocity and orientation involves cross channel comparisons that depend both on the order of the inputs and their relative geometric definitions. In mathematical terms, the multiplication tensor is coordinate system dependent (see APPENDIX).

Order and "handedness" in coordinate systems

In this section we deal with the ordering of the inputs to the multiplication tensor. Recall that this component of our models was incorporated to deal with the inherent noncommutativity of rotations (Tweed and Vilis 1987). Because its function is to properly compensate for order effects in rotations, it should not be surprising that it must be defined for a specific order of inputs in both the components of orientation and velocity. The standard multiplication formula (Eq. 9) provided by Tweed and Vilis (1987) assumed the order found in a right-handed coordinate system (defined previously). However, because order was irrelevant in the direct path matrix model of Robinson (1982), he arbitrarily used an ordering of canal matrix rows (i.e., canals pairs) that switched the brain stem activity vector into a left-handed coordinate system.² In such a coordinate system, when the thumb of the left hand is pointed along the positive direction of the first coordinate (i.e., basis vector), the fingers will curl in the direction from the second basis vector to the third basis vector, thus establishing their order. Because our

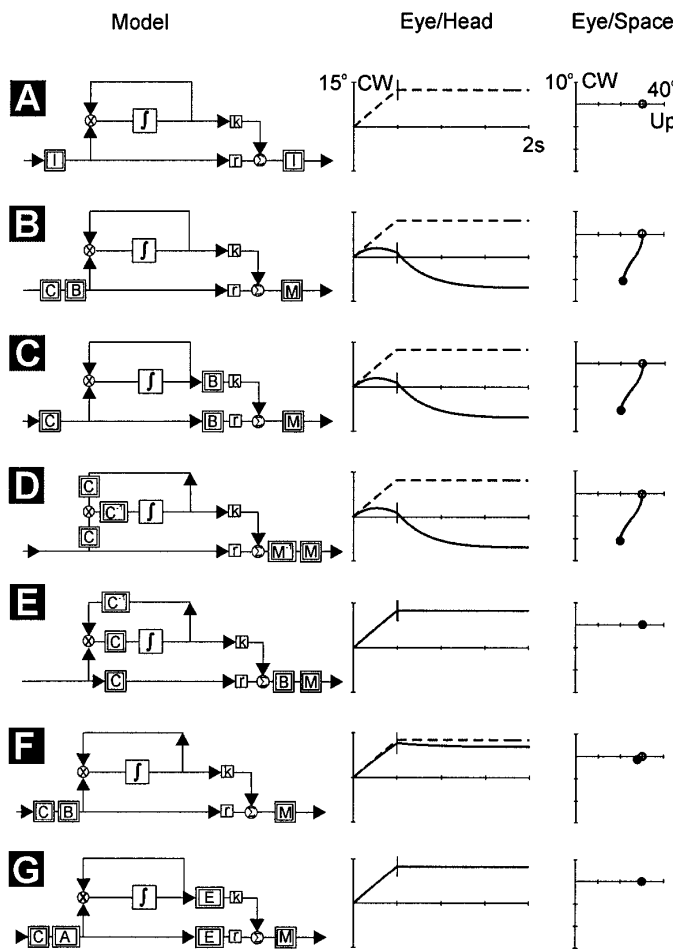


FIG. 8. Test placements of matrices for SP-matrix model. Double boxes with letters C, B, M, A, and E represent canal, brain stem, muscle, afferent, and efferent matrices, respectively. *Left column*: matrix placements. *Middle column*: resulting torsion/time for simulation 5. *Right column*: resulting eye position in space. Vertical bar indicates point at which the head stopped moving.

² Note that, although Robinson started with a right-handed x, y, z coordinate system, the placement of a single negative value along the main diagonal of his canal matrix caused a reversal to a left-handed coordinate system. Had he chosen the opposite order in his first two rows, this would not have happened.

multiplication tensor was “expecting” values in a right-handed order, it should not be surprising that, in retrospect, this formula failed in our simulations (Fig. 7 and Fig. 8, *B–D*).

Obviously, there is no inherent anatomic or physiological order between the canal pairs. What is physiologically relevant is the order of projections of the canal activity vector (and position vector) components to the multiplication tensor, and how such connections are formed. To demonstrate the contribution of this order effect to our VOR errors, we swapped the *ralp* and *rpla* from their original order in the Robinson canal matrix channels (i.e., by interchanging the 1st 2 rows), and similarly swapping the first two rows of the muscle matrix. This arbitrarily put the brain stem activity vector into a right-handed coordinate system (the biological meaning of this will be considered further in *DISCUSSION*). We then recalculated the appropriate brain stem matrix (Eq. 2) and repeated the simulation shown in Fig. 8. The results (Fig. 8, *row F*) confirmed that the order problem was indeed the major contributor to the failure in our initial quaternion-matrix models (see Fig. 7). However, this arbitrary swapping of the canal rows begs the question of how physiological systems keep established order in their inputs (this topic will be addressed in *DISCUSSION*). Moreover, although the response was now greatly improved (perhaps to within physiological tolerance), the eye still did not hold position perfectly at the end of the movement, and eye orientation in space was not yet perfectly stable.

Sensitivity to nonorthogonalities

The remaining problem in the model related to the geometric definition of the components in our brain stem coordinate systems. In addition to being defined for a right-handed coordinate system, our standard quaternion multiplication formula (Eq. 9) was defined for an orthogonal coordinate system, where the three vector components represent torsional, vertical, and horizontal values as previously defined. In contrast, our simulated brain stem activity vectors were represented in the anatomically realistic nonorthogonal coordinates provided by Robinson (1982), and thus the expected geometric meaning of these components was violated. Although on a smaller scale, this resembled confusing two components of position, for example, horizontal for vertical. Thus it is again not surprising, in retrospect, that a formula carefully designed to take the proper components of velocity and position into account would still fail.

To quantify the integrity of the multiplication tensor as a function of coordinate nonorthogonality, we conducted the following sensitivity analysis. We started with our brain stem models in the original right-handed orthogonal coordinate system used in our control simulations (Fig. 7). We then varied the degree of orthogonality between the torsional and vertical coordinate axes [varying other combinations of axes (not shown) produced similar results]. Figure 9 shows the degree of retinal slip (quantified as eye speed in space) for 2.5° steps of nonorthogonality (up to 15°) at head rotation speeds ranging from 50 to 400°/s within a realistic oculomotor range. Figure 9A shows the traces from the SP-matrix model, whereas *B* shows the traces from the LP-matrix

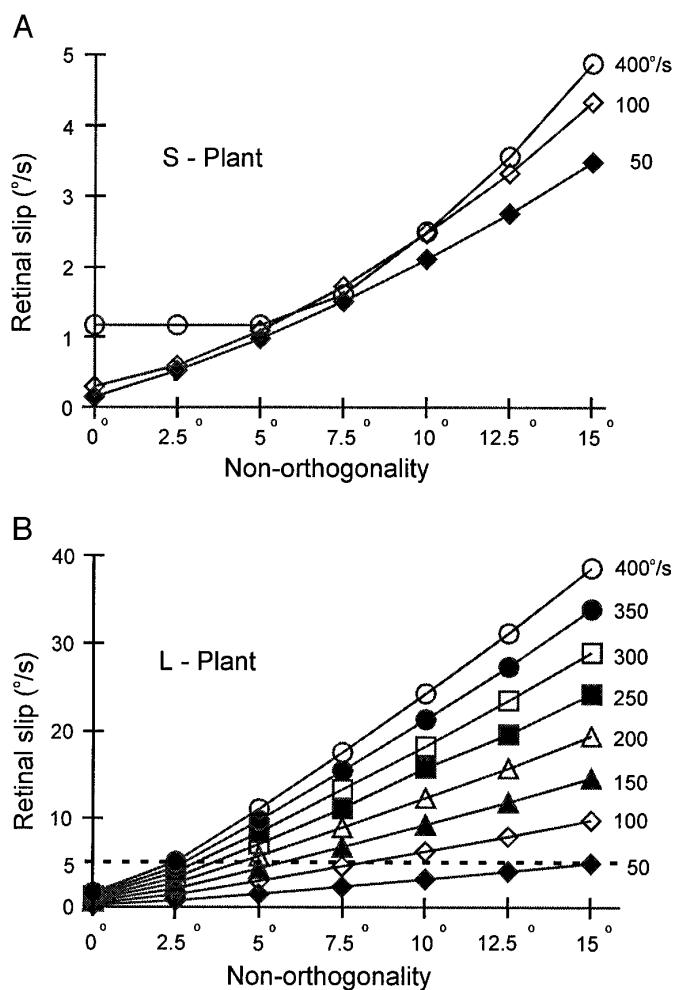


FIG. 9. Sensitivity analysis of standard tensor to varied degrees of non-orthogonality. Figure shows eye velocity in space (retinal slip) as a consequence of the degree of nonorthogonality of the torsional and horizontal axes. *A*: SP-matrix model. *B*: LP-matrix model. Note that retinal slip of the SP-matrix model does not exceed 5°/s for the tested range (see text for explanation).

model. Quantified in this way, the SP-matrix model showed a relative insensitivity to nonorthogonality because the degree of retinal slip did not exceed 5°/s within the tested range. This relatively low rate of retinal slip occurred because the errors in this model were spread out over time in a relatively slowly drifting pulse-step mismatch (see Fig. 7C). In contrast, the “muscle-pulley” LP-matrix model showed a relatively high degree of sensitivity to nonorthogonality, because its errors were actualized instantaneously. Even within 5 to 10° deviations from orthogonality, this model produced 12–25°/s speeds of retinal slip, representing a substantial loss of visual acuity. Note, however, that quantified in terms of final eye orientation, both models malfunctioned in exactly the same way.

Thus a VOR multiplication tensor defined for orthogonal coordinates could probably tolerate small physiological nonorthogonalities reasonably well, but will not tolerate larger nonorthogonalities that might result from, e.g., damage and reattachment of the muscles. Conversely, an orthogonal,

right-handed coordinate system should function reasonably well with a multiplication formula defined for a slightly different nonorthogonal coordinate system. Note that the orthogonality problem is more general than, and in fact incorporates, the order problem described above. For example, switching the order of two originally orthogonal channels can be described as a 180° non-orthogonality. In the following section, we will describe our first attempt to provide a physiologically plausible model that deals with both of these problems in a mathematically simple fashion.

Orthogonal brain stem solution

Suppose that one wanted to simulate an ideal VOR using the standard quaternion multiplication formula (Eq. 9). As demonstrated above, this would require that the operation be performed in a right-handed coordinate system. In other words, the canal afferents would have to project to this operator in a right-handed order. Furthermore, to produce ideal behavior, the brain stem coordinate system would have to be in orthogonal coordinates, for which there is some physiological evidence (Crawford 1994). Because the canal and muscle matrices are not orthogonal, this would require two brain stem coordinate transformations, one afferent (matrix A), and one efferent (matrix E), to the multiplication tensor, such that the intervening coordinates would be orthogonalized. This “orthogonal brain stem solution” is shown schematically in Fig. 8, row G (left), and as illustrated Fig. 8 (G, right) it does provide an ideal VOR.

The following section describes our method for deriving the A and E transformations. To reflect the arbitrary physiological order of the canals and muscles, we began with the left-handed ordering used by Robinson (1982). Unfortunately, these matrices could not simply be inverted to give a simple torsional/vertical/horizontal coordinate system because physiological experiments have already shown that brain stem coordinate systems are not parceled neatly into torsional and vertical centers, but rather combine these directions in much the same way as do the canals and muscles (e.g., Crawford et al. 1991). Thus we required the matrix (A) to transform the canal matrix into an orthogonal right-handed coordinate system, but rotated horizontally 45° from the original i, j, k coordinates about the k axis (Crawford 1994). The basis vectors of such a coordinate system when arranged in a matrix (X) are as follows

$$X = \begin{bmatrix} 0.707 & -0.707 & 0 \\ 0.707 & 0.707 & 0 \\ 0 & 0 & 1 \end{bmatrix} \quad (11)$$

We then noted that in any matrix coordinate transformation the original basis vectors are rotated by the inverse of that matrix (e.g., Anton and Rorres 1994). Thus the rotation of i, j, k (the identity matrix) by the inverse of C and then the inverse of A would equal X

$$X = A^{-1}C^{-1} \quad (12)$$

on rearranging we have

$$A = (XC)^{-1} \quad (13)$$

This gave the following matrix (A), which orthogonalized

the original “canal” coordinates, while leaving them rotated from Cartesian coordinates in a physiologically realistic fashion (Crawford 1994; Crawford et al. 1991; Simpson and Graf 1981)

$$A = \begin{bmatrix} 0.975 & -0.075 & -0.151 \\ 0.075 & -0.975 & 0.151 \\ 0.257 & 0.257 & 0.992 \end{bmatrix} \quad (14)$$

A similar procedure was used to compute the motor efferent matrix (E) that would transform our orthogonal brain stem coordinate system into signals appropriate for the muscles

$$E = \begin{bmatrix} 0.973 & -0.353 & -0.012 \\ -0.135 & -1.014 & -0.013 \\ -0.134 & 0.066 & 1.003 \end{bmatrix} \quad (15)$$

Note that these matrices were derived for Robinson’s left-handed canal and muscle matrices. Not surprisingly, these manipulations reestablished the ideal VOR response as illustrated in Fig. 8G. Thus the process described in Eqs. 11–15, whereby we computed the correct overall afferent and efferent projection strengths for the standard multiplication tensor, provided a relatively simple solution that was mathematically correct and in some respects biologically plausible.

Alternative tensor solution

The problem with the preceding scheme is that it implies that the system begins with a hard-wired set of local network connections that remain inflexible throughout life (the multiplication tensor), and then must learn to maintain the precise pattern of synaptic inputs to this operator thereafter. This clearly contradicts the findings of developmental neuroscience and neural network modeling, which suggest that coarse-grained, serial/parallel projections are established first in some reasonably ordered fashion, and then the precise local network connections (like those in our multiplication tensor) are fine tuned by further development and learning that remains an ongoing process throughout life (e.g., Robinson 1992). Furthermore, although orthogonal coordinates are advantageous for optimizing signal-to-noise ratios (Robinson 1985), there may be pathological situations where even approximate orthogonality is not possible (as described further in DISCUSSION). Thus the requirement that the brain stem must always develop a right-handed, perfectly orthogonal solution to satisfy the hard-wired requirements of a single operation seems unlikely, given the inherently distributed and sloppy nature of biological systems.

A more developmentally realistic solution to this problem would require that we start with some coordinate system (reflecting the serial/parallel projection weightings), and then match the formula for quaternion multiplication to these coordinates (reflecting a fine tuning of local network connections). To do this, we had to consider quaternion multiplication in a general way. As mentioned above, quaternion multiplication is an example of a tensor. Other more familiar examples of tensors are dot products and cross products. Indeed, because quaternion multiplication can be decomposed into the latter two operations (Tweed and Vilis 1987), there is nothing special about the fact that we are using quaternions here. However, some consideration of tensor

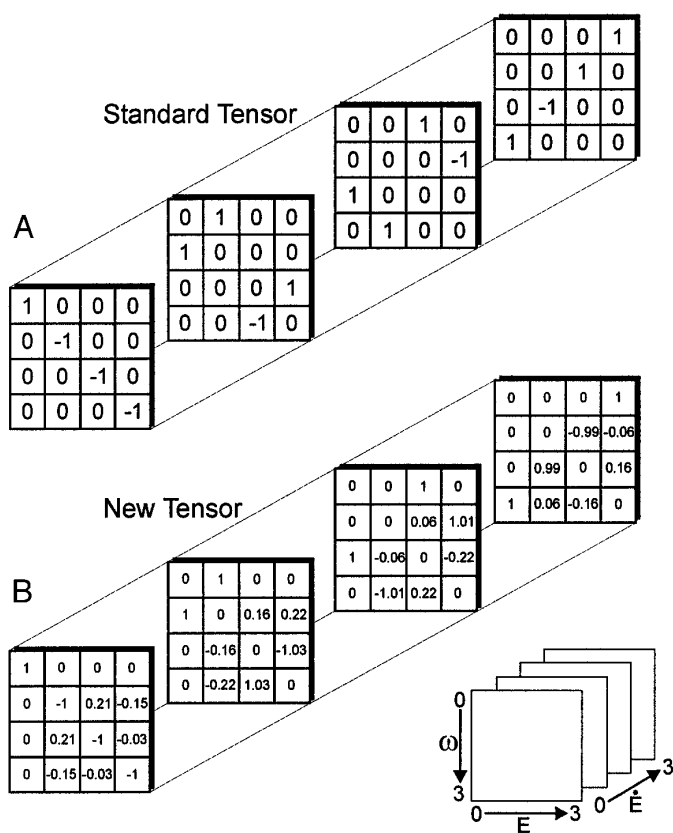


FIG. 10. Tensor coefficients for quaternion multiplication. A: standard definition of tensor formula for quaternion multiplication in orthogonal coordinates. Each element (ω, E, \hat{E}) represents an entry in the general tensor $4 \times 4 \times 4$ matrix. Usually, in the case for orthogonal coordinates, only the nonzero entries are specified. B: general definition of the tensor formula for quaternion multiplication in motor coordinates. In the general definition, each element (ω, E, \hat{E}) is specified because one cannot know beforehand which entries will be nonzero.

algebra will be required to implement these operations in nonstandard coordinates (for a more detailed mathematical explanation, see APPENDIX).

The standard formula for quaternion multiplication (Eq. 9) is actually a simplified version of a more complex tensor with all of the irrelevant coefficients deleted. The complete 64-component tensor for orthogonal coordinate systems is illustrated in Fig. 10A. Each component of this tensor establishes the relationship between each component of each input and each output (one can conceptualize these as overall synaptic weightings between the various components). A 64 ($4 \times 4 \times 4$) component tensor is thus required because there are two four-component inputs and one four-component output [because the 0th component of one input (ω) is always equal to 0, the top rows of the tensor elements in Fig. 10 can effectively be eliminated, leaving a 48-component operator]. In the standard tensor (Fig. 10A) there are numerous zeros that are not shown in the standard formula (Eq. 9). However, these components become nonzero and therefore important in nonorthogonal coordinates.

Tensor algebra was useful in this situation because it allowed us to compute the components of a general tensor to conduct multiplicative operations in arbitrary coordinates

(see APPENDIX for details). For illustrative purposes, we began by computing the tensor for the left-handed nonorthogonal ‘‘motor coordinates’’ used in Fig. 7. Figure 10B shows the resulting tensor, which has numerous new nonzero components. In practice, this was computed at the start of each simulation and then used as the quaternion multiplication formula during the simulation. That is, the quaternion representing velocity (ω) and the quaternion representing estimated eye position (E_m^*) were multiplied according to the coefficients contained in the tensor matrix.

The responses of the new tensor model were indistinguishable from the control responses (Fig. 3) of an ideal VOR for all simulations, including situations with extremely high head velocities and exaggerated oculomotor ranges (not shown). The response of the new model to standard simulation 5 is illustrated in Fig. 11. The solid lines show the incorrect response of the SP-matrix (left column) and LP-matrix (right column) models, whereas the dashed line shows the correct response of the new model. Figure 11,

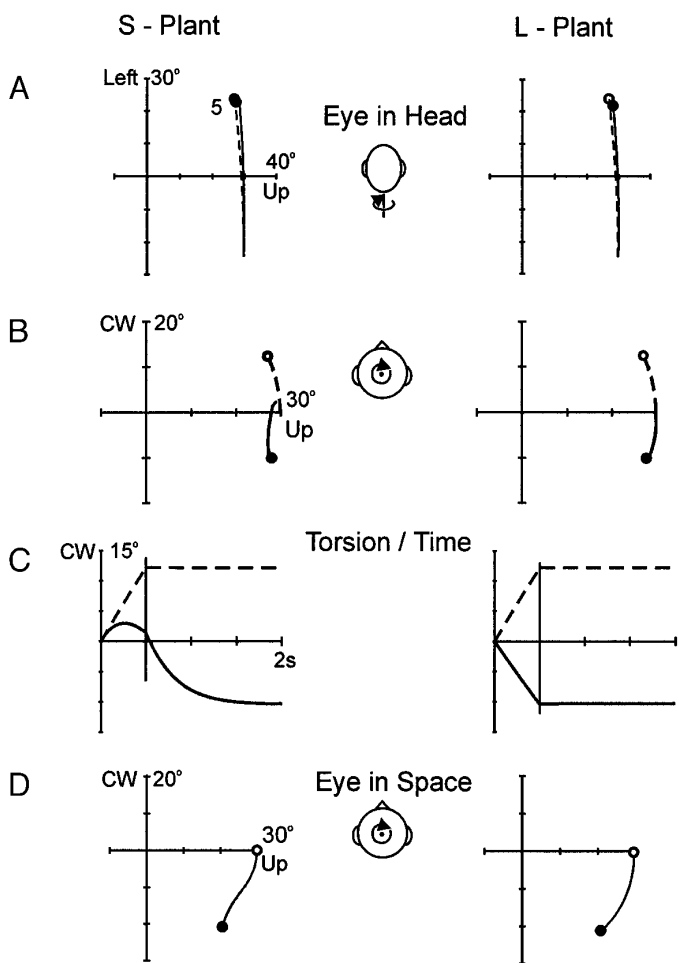


FIG. 11. Comparison of SP and LP-matrix model responses with new tensor model response. Incorrect response of the SP and LP-matrix models (solid lines); correct response of the new tensor model (dashed lines) for simulation 5 (see Fig. 3); left column, SP-matrix model; right column, LP-matrix model. A: eye position in head, behind view. B: eye position in head, above view. C: torsion vs. time. D: eye position in space. ●, final, incorrect, eye position of the matrix models. ○, final, correct, eye position of the new tensor model.

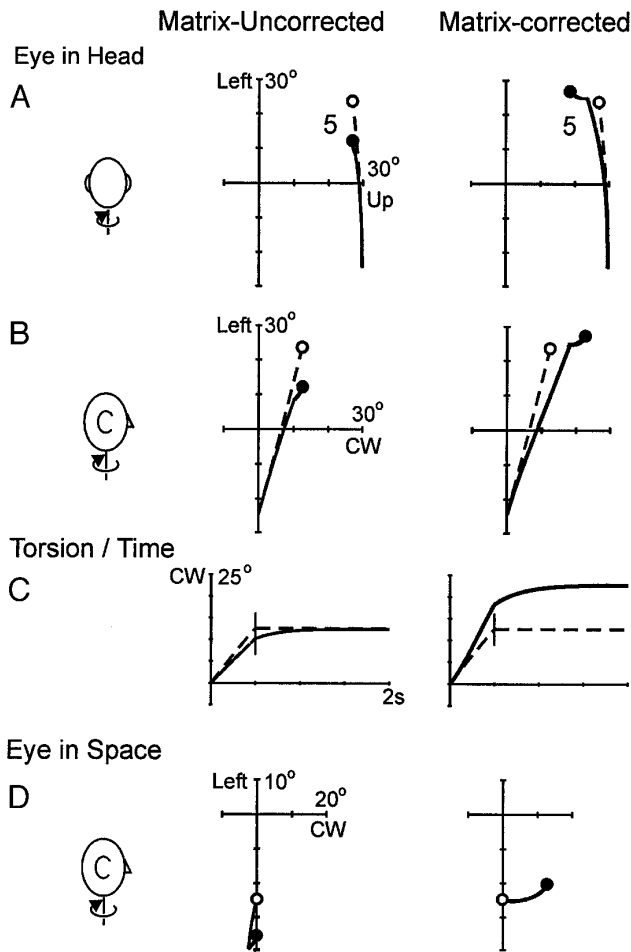


FIG. 12. Response to 50% weakening of the lateral and medial rectus muscles (SP-matrix model) to *simulation 5* (see Fig. 3). Incorrect response of SP-matrix model (—); correct response of new tensor model (---). *Left column*: response with no brain stem matrix correction. *Right column*: response with brain stem correction (see text for explanation). *A*: behind view of eye position in head (horizontal/vertical). *B*: side view of eye position in head (torsion/horizontal). *C*: torsion/time. *D*: eye position in space.

row *A*, shows eye-in-head-position from the behind view. The solid lines illustrate that the horizontal and vertical eye trace of the uncorrected models showed similar errors to those shown in Fig. 7. With the inclusion of the tensor, however, the models output the ideal response as illustrated by the dashed lines. Row *B* shows the above view, which highlights the incorrect torsional behavior of the models (solid lines), whereas the correct behavior output by the tensor model is shown by the dashed lines. Torsion over time (row *C*) was also incorrect for both original matrix models but is ideal and stable for the new tensor model. As a result of the incorrect eye-in-head behavior, gaze in space (row *D*) was not stable for the models without the corrected tensor (solid lines and ●), whereas gaze in space was ideal for the new tensor models (○). Thus the new tensor model performed an ideal VOR while using arbitrary coordinates.

The placement of the brain stem matrix was now somewhat arbitrary because it could be placed downstream of the multiplication step, although this would require the calcula-

tion of a new tensor for sensory coordinates, since the coordinate transformations occurring upstream are not the same. Indeed, the strength of the tensor solution was that it worked with left-handed, right-handed, orthogonal, or nonorthogonal coordinates with equal ease. In other words, the advantages of the orthogonal brain stem solution could be combined with the advantages of the tensor solution.

Adaptation to muscle damage

Suppose that the correct tensor had been set, as described above, for whatever coordinate system the brain used. Our previous analysis (Figs. 8*F* and 9) indicated that the system would be reasonably tolerant to small day-to-day changes in neural coordinates (e.g., Crawford 1994), but how would it respond to larger coordinate changes that might accompany system damage? We were now in a position to test Robinson's assertion that canal or muscle damage could be corrected simply by recalculating the elements of a single brain stem matrix (Robinson 1982). Such a recalculation

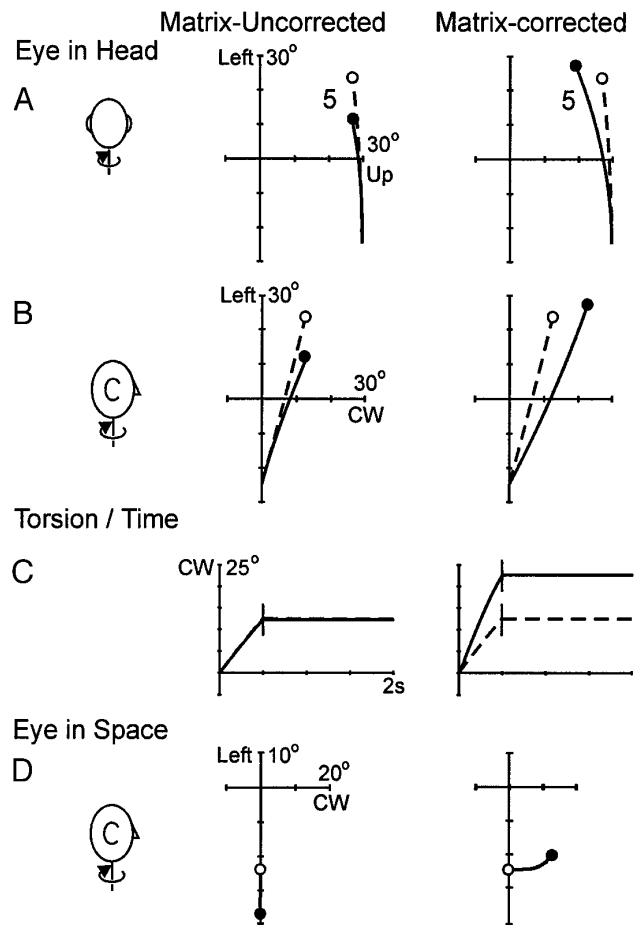


FIG. 13. Response to 50% weakening of the lateral and medial rectus muscles (LP-matrix model) to *simulation 5* (see Fig. 3). Incorrect response of SP-matrix model (solid lines); correct response of new tensor model (dashed lines). *Left column*: response with no brain stem matrix correction. *Right column*: response with brain stem correction (see text for explanation). *A*: behind view of eye position in head (horizontal/vertical). *B*: side view of eye position in head (torsion/horizontal). *C*: torsion/time. *D*: eye position in space.

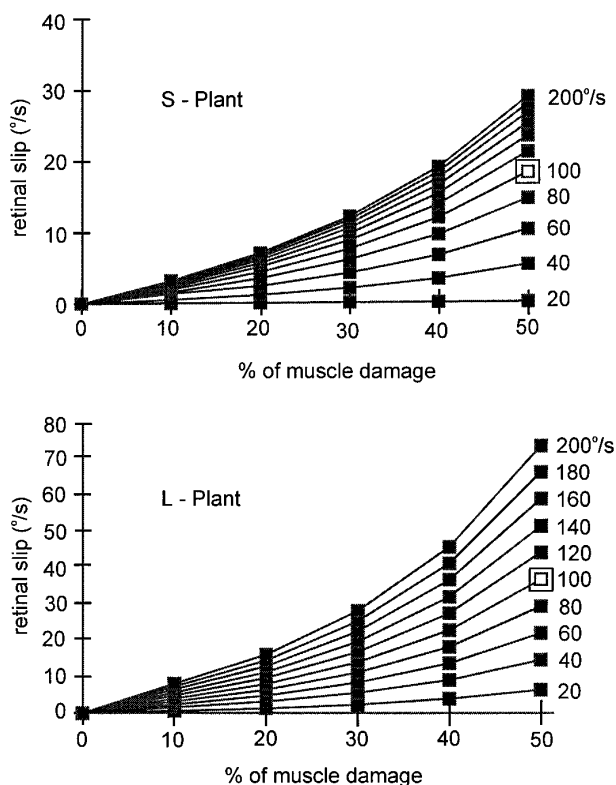


FIG. 14. Degree of retinal slip (eye velocity in space) as a function of muscle damage and rotational head speed. A: SP-matrix model. B: LP-matrix model. Note that the LP-matrix model produces approximately twice the retinal slip of the SP-matrix model. Data points are displayed for 10 different head speeds ranging from 20 to 200°/s in 20°/s increments. Open square around the data point at 50% muscle damage and 100°/s head velocity represents the simulation illustrated in Figs. 12 and 13.

suggests that an adjustment of the projection weights between the nuclei involved in the VOR would be sufficient to compensate for damage to the system. We tested this hypothesis for muscle damage with the brain stem in motor coordinates (brain stem matrix upstream from the multiplication tensor).

Figure 12 shows the responses obtained from the SP-matrix model (with an initially correct tensor). For simplicity, the actions of both the lateral and medial rectus muscles were weakened by 50% (accomplished by multiplying the 'l_{mr}' column of the muscle matrix by 0.5). Similar simulations with the LP-matrix model are shown in Fig. 13. The *left column* (solid lines) shows the results of the SP-matrix model with the elements of the single brain stem matrix uncorrected, whereas the *right column* shows this model with the elements of the single brain stem matrix corrected to compensate for the muscle damage. The dashed lines in both the *left* and *right columns* show the ideal response. Looking first at the *left column* (brain stem matrix uncorrected), the behind view (*row A*) shows that the main effect of the damage was to reduce the horizontal component (*left trace*) of eye position. In *row B*, the torsional versus horizontal plot shows a sluggish torsional response when compared with the ideal response (dashed line). The torsion versus time plot (*C*) shows that after the head stopped (vertical bar), eye position continued to change inappropriately.

The consequence of these incorrect eye in head positions is that the eye is no longer held stable in space (*row D*).

When we followed Robinson's suggestion and corrected the elements of a single brain stem matrix to compensate for damage the muscle damage (Fig. 13, *right column*), the model still failed to give a correct response. The resulting response overcompensated in all directions, including a large and inappropriate torsional movement. This occurred because the adjustments to a single brain stem matrix rendered the originally correct multiplication tensor incorrect for the new coordinates now defined by that new brain stem matrix. Thus the ideal response was achieved only when both the brain stem matrix *and* the tensor were recomputed (---).

The dramatic results of the previous simulations were particularly surprising because we only weakened one muscle pair without altering the orthogonality of the muscle (and hence brain stem) coordinates. Indeed, this touched on the third and final problem for matching the multiplication tensor to its coordinates: normality. Robinson's canal and muscle matrices were orthonormal, meaning that each of the three canal pairs/muscle pairs had the exact same sensitivity/strength. In reality, this is unlikely to be true. For example, the horizontal recti are thought to be considerably stronger than the other muscles. Figure 14 shows a sensitivity analysis similar to Fig. 9, except now the retinal slip associated with the standard multiplication tensor is quantified as a function of 10% steps in decreasing horizontal recti strength, with concomitant Robinsonian adjustments in an upstream brain stem matrix. As shown, this poses a major practical problem for the notion of a fixed tensor in Robinsonian coordinates.

Of course, the preceding sections rely on Robinson's assumption that there is a single brain stem matrix. In such simulations both the type of damage (canal or muscle) and the placement of the brain stem matrix are important because the tensor required for correct system operation depends on the upstream coordinate transformations that shape its input

TABLE 1. Effects of the different placement of matrices on the multiplicative interaction

	Transform Downstream	Transform Upstream	Both Transformations
Control	C ⊗ B M	C B ⊗ M	C A ⊗ E M
Muscle damage	C ⊗ B' M'	C B' ⊗ M'	C A ⊗ E' M'
Canal damage	C' ⊗ B' M	C' B' ⊗ M	C' A' ⊗ E M

The differing placement of the multiplicative step requires that one or more matrices be modified, depending on the location of damage to the system. In the case of a single brain stem matrix (2 left columns), a change in the tensor will also be required if the matrix upstream from the multiplicative step is modified. For example, with muscle damage and the transform upstream from the multiplicative step (⊗), the brain stem matrix must be modified in order for the combined output of the canal and brain stem matrices to deliver the input expected by the muscle matrix. This in turn forces the tensor (located within the multiplicative step, ⊗) to be redefined, because its input (the modified brain stem matrix, B') has changed. In the right column, only the matrices must be changed in response to damage because they maintain the coordinate system for which the tensor was originally defined. C, canal matrix; B, brain stem matrix; M, muscle matrix; C', modified canal matrix; B', modified brain stem matrix; M', modified muscle matrix; A, afferent matrix; E, efferent matrix; A', modified afferent matrix; E', modified efferent matrix.

(Table 1). For example, we also simulated canal damage (not shown) with the brain stem in sensory coordinates (brain stem matrix downstream) and obtained similar results. However, the orthogonal brain stem solution offers a different solution to canal/muscle damage, because it uses both afferent (A) and efferent (E) matrices. In the case of canal damage, recomputation of matrix (A) can reestablish both the correct gains and “orthogonality” of the brain stem, without any long-term changes in the multiplication tensor (this follows trivially from preceding sections). Similarly, muscle damage could be correctly compensated for by appropriate adjustments to matrix (E). We simulated both of these possibilities and found that they also reestablished an ideal VOR, similar to that shown in Figs. 12 and 13 (– – –). Furthermore, similar adjustments could be used to compensate for anisotropies in normal canals and muscles. The physiological implications of this, and the matrix-tensor solution (Figs. 12 and 13) will be considered below.

DISCUSSION

The current investigation suggests three important conclusions; the first specific to the VOR, but the remaining two have more general significance. First, we have shown that a tensor multiplication of eye orientation and angular velocity is required for ideal VOR function (Tweed and Vilis 1987), regardless of plant characteristics. Second, the correct function of such tensors depends on the way that they are matched to their coordinate systems. In other words, coordinate transformations effect not only serial/parallel neural projections in the brain (Pellionisz and Llinas 1980; Robinson 1982, 1985), but also the lateral connections occurring within these coordinates. Finally, because this suggests that intermediate coordinate systems may be optimized for purely local computational requirements (Crawford 1994; Masino and Knudsen 1993), the concept of a direct, progressive sensorimotor coordinate transformation is perhaps flawed. The behavioral, computational, physiological, developmental, and clinical implications of these conclusions will each be discussed in turn.

An ideal VOR requires a velocity/orientation multiplication tensor

Recent investigations have shown that an internal multiplicative comparison between eye orientation and angular velocity may not be necessary in the saccade generator, if the actual oculomotor plant behaves like the linear plant modeled in this study (Crawford and Guitton 1997; Quaia and Optican 1997; Raphan 1997, 1998). This is because the saccade-related burst neurons need not encode angular velocity, but may instead encode the derivative of eye orientation, which may be input directly to the neural integrator (Crawford 1994) and the linear plant (Tweed et al. 1994). However, it is physically impossible for the canal activity vector to encode eye orientation derivatives (Tweed 1997). Therefore the VOR cannot avoid the problem of converting angular velocity into commands for eye orientation or its derivative. Our simulations show that, contrary to the suggestions of some investigators (Demer et al. 1995; Schna-

bold and Raphan 1994), a multiplication tensor is necessary for both the SP and LP models of the VOR, i.e., its absence produced a significant degradation of vision in both models (see Fig. 4).

With the LP model, some configuration changes were required in the brain stem portion because the original Tweed-Vilis model (Tweed and Vilis 1987) (i.e., the SP model) required the multiplication tensor only within the indirect path, whereas the tensor was required in both paths of the LP model (Tweed 1997). Indeed, this made the linear plant version even more dependent on the multiplicative step (Fig. 5). Without this step (Figs. 4 and 5), the VOR showed a dramatic degradation in orientation control, stabilization of gaze direction, and in reduction of retinal slip. Previous experiments (Crawford and Vilis 1991) have already shown that this predicted pattern of errors does not occur in monkeys, but further experiments will be required to evaluate the performance and development of this process in humans.

For example, Misslisch et al. (1994) found that, in the dark, humans produced slow phase axes with a quarter-angle rule, i.e., midway between Listing’s law and an ideal VOR. This could represent a failure to completely “undo” the mechanical position dependencies in the plant (Demer et al. 1995; Optican and Quaia 1998). This is easily modeled in our linear plant VOR as a 50% underestimation of eye position in the multiplication tensor. However, even the 1-D gains observed by Misslisch et al. (1994) were ~50% of ideal, so the quarter-angle rule observed here may not represent the capabilities of the system for ideal behavior in the light. To help clarify these issues, further studies of human VOR performance in practical visual tasks would be useful.

Finally, although quaternions were used to implement the multiplicative step in our models, a number of different kinematic representations could be used with equal success (Haslwanter 1995). The real issue connected with the use of the multiplication tensor is the requirement of “cross-talk” between the coordinate channels. For example, knowledge of both the direction of head velocity (e.g., purely horizontal) and current eye position (e.g., elevated 20° from primary position) is necessary to compute the correct degree of torsion required to stabilize eye orientation, even though no torsion is being specified by the canals in this case. The component-wise nature of the multiplicative step, where each component is dependent on each of the others, is evident in the basic formula for this operation (Eq. 9). Thus the fundamental physiological observation to be made is that each component of the canal signal must be compared with each component of eye position before being integrated (Tweed and Vilis 1987).

Possible anatomic location of the multiplication tensor

The real brain, of course, need not use any mathematical functions that we would recognize. When we speak, then, of where in the brain the tensor may be set, we are referring to where the functional equivalent of the tensor in our models is accomplished in the brain. Thus, even if one was to record from single units in a “tensor center,” it would likely be difficult to recognize on a cell-by-cell basis. However, this center would need to possess signals in all three dimensions

that correlate both to angular eye velocity during head rotations and eye position (because these are the signals being multiplied). Furthermore, if the linear plant version is correct, this center would have to be functionally upstream from the neural integrators in the interstitial nucleus of Cajal (Crawford et al. 1991) and nucleus prepositus hypoglossi (Cannon and Robinson 1987). The vestibular nuclei are thus ideal candidates for the location of this function (e.g., Tomlinson and Robinson 1984).

By our definitions, the best way to show that some part of the vestibular nuclei perform the equivalent to a tensor multiplication would be to look at its input/output relations during the VOR. For example, the inputs should encode ω while the outputs should encode \dot{E} . These signals, in turn, should be differentiated by their different correlations to eye movement kinematics. For example, during head rotations about axes in Listing's plane, ω_{head} or ω_{eye} will have zero torsional components, whereas \dot{E} will have torsional components that depend on initial eye position (Crawford and Vilis 1991). In this situation, the phasic signal on the input side should encode ω independent of eye position, whereas the phasic output activity should correlate with the position-dependent torsional components of \dot{E} . Although technically difficult, such an investigation may be easier to implement than similar studies involving burst neurons (Hepp et al. 1994) because the phasic component of the vestibular signal can be sustained for a longer period to give a better signal-to-noise ratio.

Coordinate transformations affect intrinsic computations

We began our investigation with two internally consistent traditions in modeling that addressed two different aspects of the VOR. First, the Robinson matrix model (Robinson 1982) was a 3-D model of the VOR that emulated coordinate transformations in the direct velocity path. Second, the Tweed-Vilis quaternion model (Tweed and Vilis 1987) emulated an ideal VOR in 3-D space by incorporating a solution for the noncommutative nature of 3-D rotations in the indirect path. In combining both of these models to acquire a 3-D model of the VOR that used realistic coordinate systems and obeyed the principles of rotational kinematics, we found that the standard multiplication tensor required to transform angular velocity into rate-of-position change in the VOR no longer worked.

This finding suggests that any system with tensorlike operations will be coordinate system sensitive. As we have shown, unless the coordinate system is always right-handed and orthonormal, the formulas for standard tensor operations (such as quaternion multiplication, cross-products, etc.) will not work. To optimize behavior, the control system must therefore correctly match such tensors with their intrinsic neural coordinate systems. This is of particular relevance to biological systems for motor control, which must frequently deal with complex kinematic geometries (e.g., Crawford and Guitton 1997) using distributed, learning networks (Robinson 1992). We suggest that optimizing tensors for their coordinates is an important function of the physiological correlates of these networks.

Tensor algebra has previously been used to address VOR

nonorthogonalities by Pellionisz and Llinas (1980). However, despite some general relations, our use of tensor algebra is quite distinct from that employed by Pellionisz. First, we are addressing two different problems. Pellionisz was addressing the "covariant-contravariant" transformation in the direct path, whereas we have addressed a problem of rotational kinematics in the indirect path. Second, he was addressing a one-input, one-output (i.e., 1,1) tensor problem, whereas we addressed a higher order (2,1) tensor. Third, although Pellionisz's covariant-contravariant transformation is still of conceptual interest, Robinson (1982) demonstrated that it could be circumvented for certain practical purposes. Furthermore, Anastasio and Robinson (1990) argued that Pellionisz's apparent attempt to use tensor algebra to compute exact neural weightings was misguided, due to the sloppiness and redundancy of real network connections.

Our tensor description is immune to such criticisms because 1) as described above, the multiplication tensor is fundamental to the function of the VOR irrespective of the plant or intrinsic coordinate system, and 2) we make no claim that our tensor weightings correspond to individual synaptic weightings, but only that they highlight the overall weightings of comparisons between certain channels and how these depend on intrinsic coordinates. Ironically, some have argued that such tensors are unnecessarily complex (Raphan 1997), but it can be shown that they can be simplified considerably without losing their advantage over purely linear systems (Tweed 1997). More importantly, the latter argument is superfluous in real biology, in light of the enormous redundancy and subtlety of actual network connections mentioned above (Robinson 1992). However, the advantage of our algorithmic approach is that it points out fundamental computational principles that would not at all be clear from observing connectivity patterns in real or modeled networks. Finally, the tensor approach allowed us to model control of rotational kinematics in realistic biological situations, where order, orthogonality, and normality cannot be assumed.

Plasticity: tensor solution versus orthogonal brain stem solution

In deriving a solution to the problem of matching the multiplication tensor to its intrinsic coordinates, we considered two approaches: the orthogonal brain stem solution, and the tensor solution. Recall that the orthogonal brain stem solution requires the canal signal be transformed into an orthogonal coordinate system before further processing. With this solution, the multiplicative operation must always be conducted in orthogonal coordinates. Furthermore, these coordinates would have to be orthonormal such that each coordinate vector has the same length, i.e., strength of projections. This solution has the advantage of maximizing signal-to-noise ratios, and allowing for adjustments both upstream and downstream from the "preset" tensor. In contrast, the tensor solution allowed for realistic adjustment of local network connections to longer range serial projections, and fine tuning of the response regardless of the coordinate system. Furthermore, note that (in contrast to conventional mathematics) it is probably no easier for neural nets to compute the multiplication tensor for orthonormal right-handed

coordinates than for any other coordinate system. These considerations led us to the hypothesis that a realistic VOR is most likely controlled by both a dual brain stem coordinate transformation and a correctly matched tensor.

In contrast, Robinson (1982) computed a single brain stem matrix and suggested that adjustments to this matrix would be sufficient to correct for damage to the canals or muscles. However, we have now shown that this potentially causes a new problem (tensor-coordinate mismatch) when rotational kinematics are considered, depending on the location of these adjustments relative to the multiplication tensor, and to a lesser degree on the type of plant used. The solution to this problem depends on the sites available for plasticity.

First, we will consider the orthonormal brain stem/dual brain stem matrix solution. This scheme can correct the problem with the use of specific afferent or efferent matrix adjustments, but in effect must know which component was damaged: the canals or the muscles. To see why, let us examine the general solution of the orthonormal brain stem. With muscle damage the general solution is

$$CA \otimes E'M' \quad (16)$$

where changes in the efferent matrix (E') compensate for muscle damage (M'). In contrast, with canal damage, the general solution is

$$C'A' \otimes EM \quad (17)$$

Thus, to keep the multiplicative operation in orthonormal coordinates, the system must know whether to react by modifying the response to the canals or the response to the muscles. The information about which system is damaged is not contained, however, in retinal slip. Thus this solution would require that the system correlate behavior context with the retinal slip. For example, retinal slip that is specifically associated with vestibular input would lead to adjustments in the afferent matrix (Lisberger 1988), whereas retinal slip correlated to eye movement in general would result in changes to the efferent matrix (Optican and Miles 1985).

As demonstrated in RESULTS, these modifications will only solve the damage-induced tensor-coordinate mismatch problem if they effectively reestablish the original (e.g., orthonormal) internal coordinate system. However, this could take some time. Furthermore, this may not be possible in some cases, particularly when the canal or muscle matrix is damaged to the extent that it is not invertible. Finally, it is possible that the dual matrix solution is incorrect, i.e., that the sites for VOR plasticity are too limited (Lisberger et al. 1994). For these reasons, it is parsimonious to predict that the multiplication tensor will also show plasticity, such that it can be rematched to the new coordinate system.

Thus the real issue here is where the brain allows plasticity to occur. In their individual forms, the tensor solution and orthonormal brain stem solution place restrictions on plasticity that are probably both unnecessary and unbiological. By allowing plasticity to occur both within the afferent/efferent coordinate transformations and in the intervening tensor, one allows for a system that can optimize both coordinate transformations and tensor operations for their own separate ends, while ensuring that they both match as discussed above. Indeed, another possible mathematical step (which we did

not pursue) would be to combine the quaternion multiplication tensor and the afferent A matrix from the orthonormal solution into one single tensor computation, reflecting the idea that serial and lateral connections could be fine-tuned simultaneously. In such a case, the basic projections for the coordinate transformations and tensor operations would be set during development, and then be continually fine tuned and optimized throughout life. However, this does not require that the brain has any explicit knowledge of tensor algebra (Pellionisz and Llinas 1980). Because tensor malfunction or mismatch leads to retinal slip (Figs. 5 and 8), and because the pattern of this retinal slip will depend on eye position in a characteristic fashion (Figs. 4 and 7), then the tensor could be optimized simply by adjusting the appropriate connections until retinal slip is reduced, via the well-known context-dependent mechanisms of visual calibration of the VOR (Collewyn et al. 1983; Gonshor and Mellville-Jones 1973; Miles and Braitman 1980; Miles and Eighmy 1980; Lisberger and Miles 1980; Lisberger et al. 1984). The ultimate adaptive capacity of these processes would be put to the test following canal/muscle damage, where changes in the normality, and perhaps orthogonality, of these coordinates may occur.

Physiological correlates

To recalculate the tensor, the tensor network would require access to retinal slip information. This also makes the vestibular nuclei the ideal site, because they contain target neurons receiving projections from floccular areas that possess such information and are thought to be involved in VOR optimization (Lisberger 1988; Lisberger et al. 1994; Robinson 1976). If the cerebellum does indeed serve as a "teacher" for the VOR, this would implicitly entail setting the correct multiplication tensor for a given coordinate system. Other floccular target neurons could be involved in setting the afferent brain stem matrix, in line with the current view of gain adjustments of the VOR (Lisberger et al. 1994). In contrast, the optimal site of plasticity for the efferent matrix would be the synaptic inputs to the ocular motoneurons themselves (Optican and Miles 1985; Vilis and Tweed 1988), which are less understood.

To test these hypotheses, it will be necessary to rigorously evaluate brain stem coordinates during damage and recovery. Our simulations (Figs. 12 and 13) have demonstrated the predicted 3-D pattern of limited recovery from canal/muscle damage when only a single brain stem matrix is allowed to adapt and the multiplication tensor remains set. More detailed simulations could generate the predicted progressive patterns of recovery using various combinations of a single brain stem matrix with a plastic tensor, dual plastic matrices with a set tensor, or plastic dual matrices and tensors. However, this experimental/clinical question can most simply be phrased by directly asking what happens to internal brain stem coordinates during recovery. For example, the 3-D pattern of oculomotor drift during integrator failure has been used to suggest that integrator population coordinates are orthonormal and aligned with Listing's plane (Crawford 1994). Similar procedures could be used to follow the progressive changes in brain stem coordinates before, during,

and after recovery from canal damage. The question is, would the original coordinate system be reestablished (as in the orthonormal brain stem solution), and if not, would this result in the symptoms of tensor-coordinate mismatch (Figs. 12 and 13)?

Conclusions

In summary, the results of this investigation detail the need for a multiplicative tensor interaction between angular eye velocity and position regardless of the plant used. As we have shown, the neural correlates of this tensor must be matched to the order, orthogonality and the relative strength of its inputs. We offered two possible solutions to this problem: the dual matrix solution (the orthonormal brain stem being our archtypical example) and the tensor solution. The dual matrix solution consisted of an afferent matrix, possibly representing the patterns of termination of vestibular afferents within the vestibular nuclei, and an efferent matrix, possibly representing the input weightings to motoneuron outputs. This implies an important departure from the idea of a trivial progression from sensory to motor coordinates because it allows the brain stem to optimize intermediate coordinate systems for strictly local considerations, independent of peripheral anatomic geometries. In contrast, the tensor solution involved the calculation of a general tensor that allowed the kinematic interaction between angular velocity and position to be conducted under arbitrary coordinates. This solution suggests that recovery from anatomic damage to the VOR requires both an adjustment of gain through the serial projections *between* nuclei and the adjustment of the neural nets *within* nuclei. However, these two approaches need not remain distinct: we hypothesize a dual matrix-tensor approach to learning and maintaining the VOR.

APPENDIX

This discussion is drawn from a number of sources. There are many text books that discuss tensor algebra. The following may be helpful: Bowen and Wang (1976); Dodson and Poston (1991); Young (1992).

Tensors

Tensors are multilinear functions. This means that if any one of the tensor's inputs is allowed to vary and all the rest are held constant, then the output is a linear function of the varying input. For example, ordinary multiplication is a tensor, because if either factor is held constant, the product is a linear function of the other factor. Examples of some particular tensors are linear transformations, dot, and cross products, as well as quaternion multiplication. To review tensors we will need some terminology.

COVECTORS. We generally use the word "vector" to refer to directed magnitudes (line segments). However, vectors are actually objects that obey certain axioms. The set of such objects is called a vector space and the elements are called vectors. For example, the set of all polynomials with degree ≤ 2 form a vector space, as does any Euclidean space of any dimension.

Given any vector space, covectors are the linear functions from the vectors to R^1 . Sums and scalar multiples of covectors ϵ and φ can be defined as

$$\begin{aligned} (\epsilon + \varphi)(v) &= \epsilon(v) + \varphi(v) \\ c\epsilon(v) &= c \cdot \epsilon(v) \end{aligned} \tag{A1}$$

Given an ordered basis of vectors e_j ($j = 1$ to n , the dimension of the linear space of the vectors), the following correspondence between vectors and covectors define the dual basis ϵ^i ($i = 1$ to n)

$$\epsilon^i e_j = \delta^i_j \tag{A2}$$

The left-hand side indicates the output of the i th covector in the dual basis acting on the j th vector in the basis. The right hand side is the Kronecker delta, which equals 1 when $i = j$ and equals 0 otherwise. Thus the i th element of the dual basis is the unique covector that takes e^i to 1 and takes all the other vectors in the basis to 0. Note that *each* element of the dual basis depends on *every* vector in the basis, so that changing the basis by altering only the i th vector, in general gives a new dual basis with all the covectors changed.

The interaction between a vector and a covector produces a real number. This interaction can be characterized by saying that the covector acts on the vector to produce the number. But we could also say that the vector acts on the covector, i.e., the vector is a function taking covectors to real numbers. If we look at things this way, then a vector is a linear function from covectors to real numbers. In manipulating tensors, it is important to be able to switch between these two views of the relation between vectors and covectors.

If we index the components of a vector v using superscripts, and those of a covector φ using subscripts, then we have

$$v = \sum v^i e_i \quad \varphi = \sum \varphi_i \epsilon^i \tag{A3}$$

where $i = 1$ to n , the dimension of the linear space.

BASIC FORM OF THE TENSOR. An (r,s) -tensor is defined to be a multilinear function that takes in r covectors and s vectors and outputs a real number. Thus, for example, a covector is a $(0,1)$ -tensor, and a vector is a $(1,0)$ -tensor. Now suppose T is a $(1,1)$ -tensor. If we input a covector and a vector, we get a real number. But if we input only a vector then we get something that takes covectors to real numbers; i.e., we get a vector. T can therefore be viewed as a linear function that takes in one vector and puts out one vector: T is a linear transformation.

COORDINATE CHANGES. Suppose T is a $(1,2)$ -tensor over a 2-D linear space. Because T is linear in each input, and because any linear function is completely specified by what it does to a basis, T is completely specified by what it does to every combination of inputs chosen from among the basis and the dual basis for the space. There are $2^{1+2} = 8$ such combinations

$$\begin{aligned} \epsilon^1, e_1, e_1 \quad \epsilon^1, e_1, e_2 \quad \epsilon^1, e_2, e_1 \quad \epsilon^1, e_2, e_2 \\ \epsilon^2, e_1, e_1 \quad \epsilon^2, e_1, e_2 \quad \epsilon^2, e_2, e_1 \quad \epsilon^2, e_2, e_2 \end{aligned} \tag{A4}$$

Notice that covector inputs are always listed before vectors, but the order among the vectors and covectors (if there are more than one) in the combination matters. We define the ijk th component of T with respect to the basis e_i as

$$T^i_{jk} = T(\epsilon^i, e_j, e_k) \tag{A5}$$

If we switch from a basis e_i to a basis f_i , then we also switch from a dual basis ϵ^i to a dual basis φ^i . Because each new basis vector is uniquely expressible as a linear combination of the old basis vectors, there is n^2 real numbers a_j^i such that

$$f_j = a^i_j e_i \tag{A6}$$

Similarly, each new dual basis covector is uniquely expressible as a linear combination of the old dual basis covectors, and so there are n^2 real numbers b_j^i such that

$$\varphi^i = b_j^i \varepsilon^j \quad (\text{A7})$$

Tensor for quaternion multiplication required a 64-element matrix

Quaternion multiplication is a (1,2)-tensor over the 4-D space of quaternions. Thus the dimensionality of quaternion multiplication is $4^{1+2} = 4^3 = 64$. The general tensor for quaternion multiplication, then, can be specified in a $4 \times 4 \times 4$ or 64-element matrix (Fig. 10). The formula used to generate the general tensor matrix for quaternion multiplication (QM) is given by

$$\text{QM}(xyz) = \sum b(x,i)a(j,y)a(k,z)\varepsilon(i,j,k) \quad (\text{A8})$$

where i, j, k, x, y, z run from 0 to 3 (the dimension of the linear space); b is an element in a 4×4 change of basis matrix; a is an element in the inverse of the 4×4 change of basis matrix; and ε is the Levi-Civita symbol. It can be shown that the value defined by the Levi-Civita symbol equals 0 if any two of i, j, k are identical; 1 if i, j, k is a cyclic permutation of 1,2,3 (i.e., if i, j, k is 1,2,3 or 2,3,1 or 3,1,2); and -1 otherwise. The Levi-Civita operator is applied to the tensor defined, in this case, for orthogonal coordinates (given by Eq. A8).

As an example, we will discuss how to calculate the values for the tensor defined in motor coordinates (illustrated in Fig. 10B). To move from orthogonal spatial coordinates to motor coordinates, we must go through the linear transformation defined by the composition of the canal (C) and brain stem (B) transformations (found by multiplication of the matrices, i.e., $C \times B$). We should also note that the matrix A with the ij th element a_j^i (Eq. A6) and matrix B with the ij th element b_j^i (Eq. A7) are inverses of one another. Thus the motor transformation defined by $(C \times B)$ is defined in the dual basis as $(C \times B)^{-1}$. Armed with these facts, we can now apply our formula for finding a new tensor (Eq. A8). This is most easily done with a computer subroutine comprising of six nested For/Next loops where the indices of the loops run from 0 to 3.

We thank D. Tweed for critical comments and an illuminating introduction to tensors and T. Vilis for the original suggestion to combine the quaternion model with the matrix model.

This work was supported by a Canadian Natural Sciences and Engineering Research Council grant to J. D. Crawford and by the Sloan Foundation. J. D. Crawford is a Canadian Medical Research Council Scholar and an Alfred P. Sloan Fellow.

Address for reprint requests: J. D. Crawford, Dept. of Psychology, York University, 4700 Keele St., Toronto, Ontario M3J 1P3, Canada.

Received 27 February 1998; accepted in final form 14 July 1998.

REFERENCES

ANASTASIO, T. J. AND ROBINSON, D. A. Distributed parallel processing in the vestibulo-ocular reflex: learning networks compared to tensor theory. *Biol. Cybern.* 63: 161–167, 1990.

ANGELAKI, D. E. AND HESS, B. J. M. Inertial representation of angular motion in the vestibular system of rhesus monkeys. I. Vestibuloocular reflex. *J. Neurophysiol.* 71: 1222–1249, 1994.

ANTON, H. AND RORRES, C. *Elementary Linear Algebra: Applications Version* (7th ed.). Toronto: Wiley, 1994.

BLANKS, R. H. I., CURTHOYS, I. S., AND MARKHAM, C. H. Planar relationships of the semi-circular canals in man. *Acta Otolaryngol.* 80: 185–196, 1975.

BOWEN, R. M. AND WANG, C.-C. *Introduction to Vectors and Tensors*. New York: Plenum, 1976, vol. 1.

CANNON, S. C. AND ROBINSON, D. A. Loss of the neural integrator of the

oculomotor system from brainstem lesions in the monkey. *J. Neurophysiol.* 57: 1383–1409, 1987.

CHERON, G. AND GODAUX, G. Disabling of the oculomotor integrator by kainic acid injections in the prepositus-vestibular complex of the cat. *J. Physiol. (Lond.)* 394: 267–290, 1987.

COLLEWIJN, H., MARTINS, A. J., AND STEINMAN, R. M. Compensatory eye movements during active and passive head movements: fast adaptation to changes in visual magnification. *J. Physiol. (Lond.)* 340: 259–286, 1983.

CRAWFORD, J. D. The oculomotor neural integrator uses a behavior-related coordinate system. *J. Neurosci.* 14: 6911–6923, 1994.

CRAWFORD, J. D., CADERA, W., AND VILIS, T. Generation of torsional and vertical eye position signals by the interstitial nucleus of Cajal. *Science* 252: 1551–1553, 1991.

CRAWFORD, J. D. AND GUITTON, D. Visual-motor transformations required for accurate and kinematically correct saccades. *J. Neurophysiol.* 78: 1447–1467, 1997.

CRAWFORD, J. D. AND VILIS, T. Axes of eye rotation and Listing's law during rotations of the head. *J. Neurophysiol.* 65: 407–423, 1991.

CURTHOYS, I. S., HALMAGYI, G. M., BLACK, R. A., HASLWANTER, T., AND TOPPLE, A. N. Three-dimensional eye movement recordings during off-center yaw rotation of human subjects: how the linear VOR modifies the angular VOR. In: *Three-Dimensional Kinematics of Eye, Head and Limb Movements*, edited by M. Fetter, T. Haslwanter, H. Misslisch, and D. Tweed. Amsterdam: Harwood, 1997, p. 187–190.

DEMER, J. L., MILLER, J. M., POUKENS, V., VINTERS, H. V., AND GLASGOW, B. J. Evidence for fibromuscular pulleys of the recti extraocular muscles. *Invest. Ophthalmol. Vis. Sci.* 36: 1125–1136, 1995.

DODSON, C. T. J. AND POSTON, T. *Tensor Geometry: The Geometric Viewpoint and Its Uses* (2nd ed.). New York: Springer-Verlag, 1991.

GALIANA, H. L. AND OUTERBRIDGE, J. S. A bilateral model for central neural pathways in vestibuloocular reflex. *J. Neurophysiol.* 51: 210–240, 1984.

GONSHOR, A. AND MELVILL-JONES, G. Changes of human vestibulo-ocular response induced by vision reversal during head rotation. *J. Physiol. (Lond.)* 234: 102–103, 1973.

HASLWANTER, T. Mathematics of three-dimensional eye rotations. *Vision Res.* 35: 1727–1739, 1995.

HASLWANTER, T., CURTHOYS, I. S., BLACK, R. A., TOPPLE, A. N., AND HALMAGYI, G. M. The three-dimensional human vestibulo-ocular reflex; response to long-duration yaw angular accelerations. *Exp. Brain Res.* 109: 303–311, 1995.

HASLWANTER, T., STRAUMANN, D., HEPP, K., HESS, B. J. M., AND HENN, V. Smooth pursuit eye movements obey Listing's law in the monkey. *Exp. Brain Res.* 87: 470–472, 1991.

HEPP, K., SUZUKI, J., STRAUMANN, D., AND HESS, B. J. M. On the 3-dimensional rapid eye movement generator in the monkey. In: *Information Processing Underlying Gaze Control*, edited by J. M. Delgado-Garcia, E. Godeaux, and P. P. Vidal. Oxford, UK: Pergamon, 1994, p. 65–74.

HESS, B. J. AND ANGELAKI, D. E. Kinematic principles of primate rotational vestibulo-ocular reflex. I. Spatial organization of fast phase velocity axes. *J. Neurophysiol.* 78: 2193–2202, 1997.

JONES, G. M. AND GONSHOR, A. Oculomotor response to rapid head oscillation (0.5–5.0 Hz) after prolonged adaptation to vision-reversal. “Simple” and “complex” effects. *Exp. Brain Res.* 45: 45–58, 1982.

LISBERGER, S. G. The neural basis for learning of simple motor skills. *Science* 242: 728–735, 1988.

LISBERGER, S. G. AND MILES, F. A. Role of primate medial vestibular nucleus in long-term adaptive plasticity of vestibuloocular reflex. *J. Neurophysiol.* 43: 1725–1745, 1980.

LISBERGER, S. G., MILES, F. A., AND ZEE, D. S. Signals used to compute errors in monkey vestibulo-ocular reflex: possible role of flocculus. *J. Neurophysiol.* 52: 1140–1153, 1984.

LISBERGER, S. G., PAVELKO, T. A., AND BROUSSARD, D. M. Neural basis for motor learning in the vestibuloocular reflex of primates. I. Changes in the response of brain stem neurons. *J. Neurophysiol.* 72: 928–953, 1994.

MASINO, T. AND KNUDSEN, E. I. Orienting head movements resulting from electrical microstimulation of the brainstem tegmentum in the barn owl. *J. Neurosci.* 13: 351–370, 1993.

MERFELD, D. M. Modeling human vestibular responses during eccentric rotation and off vertical axis rotation. *Acta Otolaryngol. Suppl.* 520: 354–359, 1995.

MILES, F. A. AND BRAITMAN, D. J. Long-term adaptive changes in primate

- vestibuloocular reflex. II. Electrophysiological observations on semicircular canal primary afferents. *J. Neurophysiol.* 43: 1426–1436, 1980.
- MILES, F. A. AND EIGHMY, B. M. Long-term adaptive changes in primate vestibuloocular reflex. I. Behavioral observations. *J. Neurophysiol.* 43: 1406–1425, 1980.
- MILLER, J. M. Functional anatomy of normal human rectus muscles. *Vision Res* 29: 223–240, 1989.
- MISSLISCH, H., TWEED, D., FETTER, M., SIEVERING, D., AND KOENIG, E. Rotational kinematics of the human vestibuloocular reflex. III. Listing's law. *J. Neurophysiol.* 72: 2490–2502, 1994.
- OPTICAN, L. M. AND MILES, F. A. Visually induced adaptive changes in primate saccadic oculomotor signals. *J. Neurophysiol.* 54: 940–958, 1985.
- OPTICAN, L. M. AND QUAIA, C. Effects of orbital pulleys on the control of eye rotations. In: *Vision and Action*, edited by L. Harris and M. Jenkins. In press.
- PAIGE, G. D., BARNES, G. R., TELFORD, L., AND SEIDMAN, S. H. Influence of sensorimotor context on the linear vestibulo-ocular reflex. *Ann. NY Acad. Sci.* 781: 322–331, 1996.
- PELLIONISZ, A. AND LLINAS, R. Tensorial approach to the geometry of brain function: cerebellar coordination via a metric tensor. *Neuroscience* 5: 1125–1138, 1980.
- QUAIA, C. AND OPTICAN, L. M. A commutative controller is sufficient to rotate the eye. *Soc. Neurosci. Abstr.* 27: 10.8, 1997.
- RAPHAN, T. Modelling control of eye orientation in three dimensions. In: *Three-Dimensional Kinematics of Eye, Head and Limb Movements*, edited by M. Fetter, T. Haslwanter, H. Misslisch, and D. Tweed. Amsterdam: Harwood, 1997, p. 359–374.
- RAPHAN, T. Modeling control of eye orientation in three dimensions. I. Role of muscle pulleys in determining saccadic trajectory. *J. Neurophysiol.* 79: 2653–2667, 1998.
- ROBINSON, D. A. Eye movement control in primates. *Science* 161: 1219–1224, 1968.
- ROBINSON, D. A. Oculomotor control signals. In: *Basic Mechanisms of Ocular Motility and Their Clinical Implications*, edited by P. Bach-y-Rita and G. Lennerstrand. Oxford, UK: Pergamon, 1975, p. 337–374.
- ROBINSON, D. A. Adaptive gain control of the vestibulo-ocular reflex by the cerebellum. *J. Neurophysiol.* 39: 954–969, 1976.
- ROBINSON, D. A. The use of matrices in analyzing the three-dimensional behavior of the vestibulo-ocular reflex. *Biol. Cybern.* 46: 53–66, 1982.
- ROBINSON, D. A. The coordinates of neurons in the vestibulo-ocular reflex. In: *Adaptive Mechanisms in Gaze Control. Facts and Theories*, edited by A. Berthoz and G. Melvill Jones. Amsterdam: Elsevier, 1985, p. 298–311.
- ROBINSON, D. A. Implications of neural networks for how we think about brain function. *Behav. Brain Sci.* 15: 644–655, 1992.
- SCHNABOLK, C. AND RAPHAN, T. Modeling three-dimensional velocity-to-position transformation in oculomotor control. *J. Neurophysiol.* 71: 623–638, 1994.
- SEIDMAN, S. H., LEIGH, R. J., TOMSAK, R. L., GRANT, M. P., AND DELL'OSSO, L. F. Dynamic properties of the human vestibulo-ocular reflex during head rotations in roll. *Vision Res.* 35: 679–689, 1995.
- SIMPSON, J. I. AND GRAF, W. Eye-muscle geometry and compensatory eye movements in lateral-eyed and frontal-eyed animals. *Ann. NY Acad. Sci.* 20–30: 1981.
- SIMPSON, J. I. AND GRAF, W. The selection of reference frames by nature and its investigators. In: *Adaptive Mechanisms in Gaze Control. Facts and Theories*, edited by A. Berthoz and G. Melvill Jones. Amsterdam: Elsevier, 1985, p. 3–16.
- SOLOMON, D., STRAUMANN, D., AND ZEE, D. S. Three-dimensional eye movements during vertical axis rotation: effects of visual suppression, orbital eye position and head position. In: *Three-Dimensional Kinematics of Eye, Head and Limb Movements*, edited by M. Fetter, T. Haslwanter, H. Misslisch, and D. Tweed. Amsterdam: Harwood, 1997, p. 197–208.
- STRAUMANN, D., HASLWANTER, T., HEPP-REYMOND, M. C., AND HEPP, K. Listing's law for the eye, head and arm movements and their synergistic control. *Exp. Brain Res.* 86: 209–215, 1991.
- STRAUMANN, D., ZEE, D. S., SOLOMON, D., LASKER, A. G., AND ROBERTS, D. C. Transient torsion during and after saccades. *Vision Res.* 35: 3321–3334, 1995.
- TOMLINSON, R. D. AND ROBINSON, D. A. Signals in vestibular nucleus mediating vertical eye movements in the monkey. *J. Neurophysiol.* 51: 1121–1136, 1984.
- TWEED, D. Velocity-to-position transformations in the VOR and the saccadic system. In: *Three-Dimensional Kinematics of Eye, Head and Limb Movements*, edited by M. Fetter, T. Haslwanter, H. Misslisch, and D. Tweed. Amsterdam: Harwood, 1997, p. 375–386.
- TWEED, D., MISSLISCH, H., AND FETTER, M. Testing models of the oculomotor velocity to position transformation. *J. Neurophysiol.* 72: 1425–1429, 1994a.
- TWEED, D., SEIVERING, D., MISSLISCH, H., FETTER, M., ZEE, D., AND KOENIG, E. Rotational kinematics of the human vestibuloocular reflex I. Gain matrices. *J. Neurophysiol.* 72: 2467–2479, 1994b.
- TWEED, D. AND VILIS, T. Geometric relations of eye position and velocity vectors during saccades. *Vision Res.* 30: 111–127, 1990.
- TWEED, D. AND VILIS, T. Implications of rotational kinematics for the oculomotor system in three dimensions. *J. Neurophysiol.* 58: 832–849, 1987.
- VILIS, T. Physiology of three-dimensional eye movements: saccades and vergence. In: *Three-Dimensional Kinematics of Eye, Head and Limb Movements*, edited by M. Fetter, T. Haslwanter, H. Misslisch, and D. Tweed. Amsterdam: Harwood, 1997, p. 59–72.
- VILIS, T. AND TWEED, D. A matrix analysis for a conjugate vestibulo-ocular reflex. *Biol. Cybern.* 59: 237–245, 1988.
- WESTHEIMER, G. Kinematics of the eye. *J. Opt. Soc. Am.* 47: 967–974, 1957.
- WESTHEIMER, G. AND MCKEE, S. P. Visual acuity in the presence of retinal-image motion. *J. Opt. Soc. Am.* 65: 847–850, 1975.
- WESTHEIMER, G. AND MCKEE, S. P. Integration regions for visual hyperacuity. *Vision Res.* 17: 89–93, 1977.
- YOUNG, E. C. *Vector and Tensor Analysis* (2nd ed.). New York: Dekker, 1992.